



PONTIFICIA UNIVERSIDAD CATOLICA DE CHILE
INSTITUTE OF PHYSICS

PROPERTIES OF FOUR-COMPONENT
DIRAC OPERATORS DESCRIBING
GRAPHENE QUANTUM DOTS

by

Cristóbal Vallejos Benavides

A thesis submitted in fulfillment of the requirements
for the degree of Master of Sciences in Physics
at the Pontificia Universidad Católica de Chile.

Advisor : Dr. Rafael Benguria Donoso
Committee : Dr. Edgardo Stockmeyer
Dr. Hanne Van Den Bosch

December, 2020

Santiago, Chile

©2020, Cristóbal Ignacio Vallejos Benavides

©2020, Cristóbal Ignacio Vallejos Benavides

Total or partial reproduction for academic purposes is authorized by any means or procedure, including bibliographic citation of the document.

Acknowledgments

Firstly, I want to acknowledge my two advisors Professor Rafael Benguria and Professor Edgardo Stockmeyer. I appreciate their help, feedback, discussions, and willingness in these extraordinary times. In the same way, I express my thankfulness to Professor Hanne Van den Bosch for her significant contribution before realising this document. Besides, I thank their support in the application process to beginning my PhD in Physics in the United States and to the Fulbright Scholarship. All three have been strong academic figures throughout my short scientific career.

This work would not have been possible either without the help of my girlfriend, Romina Dinamarca, the love of my life. For her emotional support, moreover, her disposition to hear my ideas about this writing. In the same way, I am grateful for the help of my family, especially my mother, Patricia, for her inexhaustible understanding and comfort.

Finally, I thank my friends and colleagues:

- Mauricio Gamonal and Juan Manuel González, for their valuable companionship for the last seven years. Talks, meetings, teas, pizzas, sandwiches, table tennis afternoons and ZOOM nights.
- And all those who have helped me during my master's degree.

My work has been partially supported by Fondecyt (Chile) Projects # 116-0856 and # 120-1055.

Abstract

The electronic properties of graphene quantum dots (GQDs) can be described by the two-dimensional Dirac equation with boundary conditions consistent with the tight-binding model on a honeycomb lattice. It is convenient to know which boundary conditions are allowed by elemental physical principles of current conservation. We consider the four-component two-valley massless Dirac operator on planar domains describing GQDs. We show how to reduce the problem into the study of the two-component Dirac operator. For a large class of boundary conditions, not including the zigzag orientation, we give a proof of their self-adjointness for four-component spinor wave functions in the Sobolev space H^1 . In particular, in each case, we find a lower bound to the spectral gap around zero, proportional to the inverse of the square root of the area of the domain and depending only in the mixing angle. We also discuss the boundary conditions conserving (breaking) the electron-hole and time reversal symmetries.

Contents

1	Introduction	1
1.1	Tight-binding model on a honeycomb lattice	3
1.2	Boundary Conditions	6
1.3	Definitions and Notation	8
2	Two-valley Dirac operator with boundary conditions	10
2.1	One-Valley Description	10
2.2	Two-Valley Description	13
2.3	Boundary Matrix M	14
3	Unitary Equivalence	17
3.1	Main Theorem Proof	19
4	Symmetries	23
5	Discussion and conclusions	28
A	Mixing Matrices for the electron-hole and time reversal symmetries	30
A.1	Electron-hole Symmetry	30
A.2	Time Reversal Symmetry	33
B	Parity and Charge Conjugation Symmetries	36
B.1	Parity	36
B.2	Charge Conjugation	38
C	Symmetries on Carbon Nanotubes	40
C.1	Electron-Hole Symmetry	43
C.2	Time Reversal Symmetry	43

C.3	Charge Conjugation	44
C.4	Parity	44
C.5	Pseudo-Spin-Flip Symmetry	44
D	Technical Lemmas	46
D.1	General Considerations	47
D.2	The Unit Circle	50
D.3	Riemann Mapping and the Self-adjointness Proof	54
D.4	Spectral Gaps of Dirac Hamiltonians	56
	Bibliography	61

Chapter 1

Introduction

In this thesis, we study Dirac operators describing energy excitations in graphene quantum dots for a four-component wavefunction prescription. The results obtained here are an extension of the works of Rafael Benguria, Edgardo Stockmeyer, Hanne Van den Bosch and Søren Fournais [13, 14] realized for the two-component case. This document is in collaboration with the first three authors of those works. The thesis includes more details and possible extensions of an article in progress.

Graphene is a two-dimensional layer of carbon atoms shaping a honeycomb lattice. It was first studied in 1947 by Wallace [49] as a two-dimensional toy model of a single layer of graphite. The early interest in graphene was to find a relationship with the ultrarelativistic form of the single-particle electron spectrum. Its electronic properties can be described by a difference equation [49], or by a differential equation [21]. The tight-binding model represents the first, and the two-dimensional Dirac equation describes the second. Both descriptions are equivalent at large length scales and low energies. For 3D multilayer graphene, the Dirac equation is also known as Weyl-Dirac equation.

The experimental isolation of graphene sheets in the free states was obtained in 2004 [36], which was awarded the 2010 Nobel prize in physics. The amazing properties of graphene, such as extraordinary conductivity of heat and electricity, resistance and malleability, have attracted much interest due to its possible applications. See, e.g. [20, 26] for a complete review.

The Dirac equation was mostly applied to described neutrinos [16]. This differential equation needs to be supplement by boundary conditions consistent with the tight-binding model on a honeycomb lattice. They are necessary to know the behavior of the electron (or hole) near an edge of a sample for the description of several effects, including the anomalous quantum Hall

effect [1, 2]. In particular, it is convenient to know what boundary conditions on the Dirac equation are allowed by elemental physical principles of current conservation, (preservation or breaking of) T-symmetry and electron-hole symmetry. This problem was solved in [3, 4].

On a bounded domain $\Omega \subset \mathbb{R}^2$ with C^2 -boundary $\partial\Omega$, the dynamic of a graphene sheet is described by the Dirac Hamiltonian¹ [24]

$$H = \begin{pmatrix} T & 0 \\ 0 & T \end{pmatrix} \quad \text{on } \mathcal{H} \oplus \mathcal{H}, \quad (1.1)$$

where $\mathcal{H} = L^2(\Omega, \mathbb{C}^2)$, the space of square-integrable functions, and T is the massless one-valley Dirac operator

$$T = -i\hbar v_F \boldsymbol{\sigma} \cdot \nabla$$

acting on a dense subspace of \mathcal{H} . We write $\boldsymbol{\sigma} = (\sigma_1, \sigma_2)^T$ as the vector of the usual first two Pauli matrices. The direct sum in (1.1) is taken between two valleys with two-component wavefunctions each one. The constant v_F refers to the Fermi velocity in graphene, depending on natural constants, the hopping energy between nearest neighbors carbon atoms and the interatomic space between them, with value $\approx 10^6$ m/s⁻¹.

More specifically, we study graphene on a regime such that is large enough to use the description by the continuum Dirac operator but small enough to observe effects related to the confinement of electron on a domain. Graphene quantum dots, a localized quantum system, satisfy those both requirements. The diameter of a graphene quantum dot is about a few dozen nanometers, which is large compared to the interatomic space of 0.1 nm between the carbon atoms.

In chapter 2, we study the appropriated local boundary conditions for two-component and four-component Dirac operators. In particular, we deduce the mathematical structure of boundary matrices for boundary conditions with current conservation. In chapter 3, we present our main theorem and the proof of this through unitary equivalence. In Theorem 3.1, we establish the conditions of self-adjointness of the Dirac operator and its spectral gap energy around zero.

In chapter 4 we discuss the implication of our main theorem in the presence of two relevant physical symmetries, the electron-hole and time reversal symmetries. A more detailed deriva-

¹Also there exist other unitarily equivalent prescriptions of the Dirac Hamiltonian (see, e.g. [20, 32, 47]) to study graphene sheets, nanoribbons and carbon nanotubes with different convention orders of the spinor components of both valleys and sublattices.

tion of those boundary conditions for both symmetries is presented in Appendix A. In Appendix B we discuss charge conjugation and parity symmetry. Moreover, in Appendix C, we expound the main mathematical and physical properties of carbon nanotubes, and we deduce the corresponding symmetries. Finally, Appendix D presents technical Lemmas and Propositions of the proof of our main theorem.

The rest of this introduction we discuss the electronic excitations on the tight-binding model on a honeycomb lattice, the most used boundary conditions in the physics literature, and the notations and conventions used henceforth.

1.1 Tight-binding model on a honeycomb lattice

We start reviewing the electronic states of a graphene sheet. Figure 1.1 show the lattice structure of graphene. The honeycomb lattice is not a Bravais lattice; it corresponds to a superposition of two triangular lattices, named sublattices A (red) and B (blue). It is completely determined by two primitive lattice vectors $\mathbf{a}_1, \mathbf{a}_2$ and a unit cell containing two carbon atoms, one per sublattice.

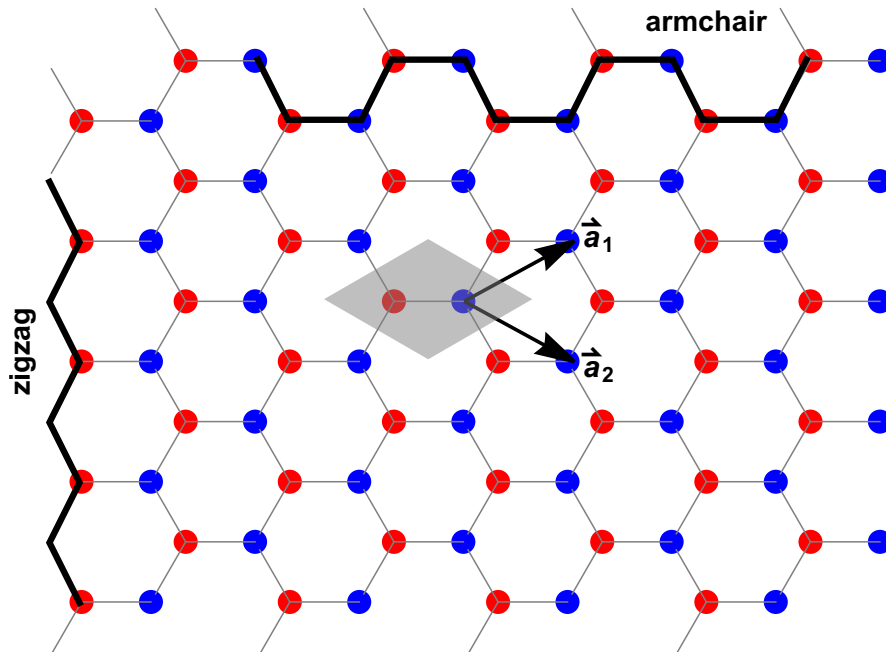


Figure 1.1: Graphene sheet in real space, where the red (blue) circles mean an A(B) sublattice site; $\mathbf{a}_1 = a/2(\sqrt{3}, 1)^T$ and $\mathbf{a}_2 = a/2(\sqrt{3}, -1)^T$ are the primitive vectors. The primitive unit cell is shaded in gray.

We choose the convention of primitive lattice vectors

$$\mathbf{a}_1 = \frac{a}{2}(\sqrt{3}, 1)^T \quad \text{and} \quad \mathbf{a}_2 = \frac{a}{2}(\sqrt{3}, -1)^T, \quad (1.2)$$

such that $|\mathbf{a}_1| = |\mathbf{a}_2| = a$ with $a \approx 2.46 \text{ \AA}$ the lattice constant². Each point on the both periodic sublattices of Figure 1.1 can be described by $\mathbf{R} = m\mathbf{a}_1 + n\mathbf{a}_2$ where m and n are two integers, where the related sublattice site inside the unit cell is taken as the origin.

The corners of the first Brillouin zone in the Figure 1.2, the unit cell in the reciprocal (momentum) space, are called \mathbf{K} and \mathbf{K}' points. They are given by

$$\mathbf{K} = \frac{2\pi}{3a}(\sqrt{3}, 1)^T \quad \text{and} \quad \mathbf{K}' = \frac{2\pi}{3a}(\sqrt{3}, -1)^T. \quad (1.3)$$

The remaining corners can be obtained as a result of a translation in the reciprocal lattice vectors \mathbf{b}_1 and \mathbf{b}_2 .

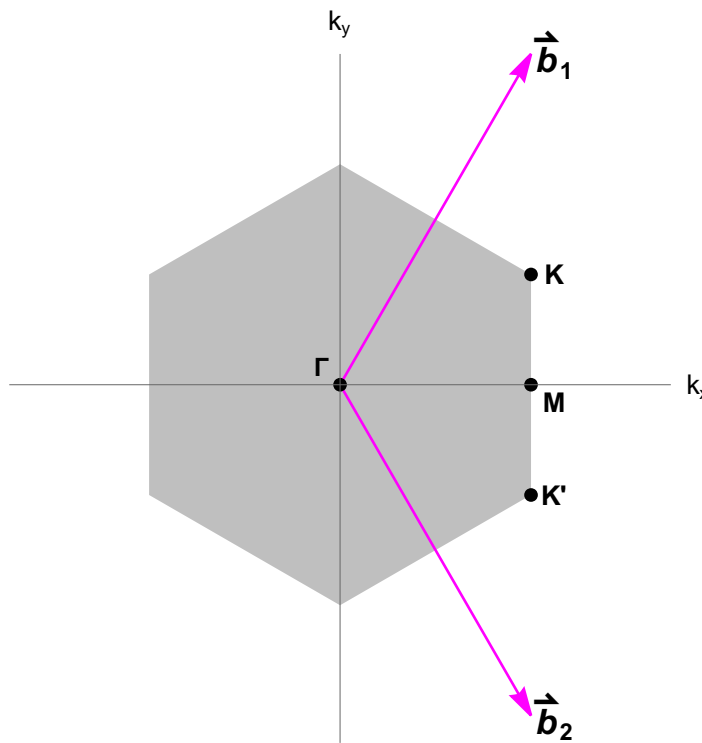


Figure 1.2: The hexagonal first Brillouin zone (reciprocal space) of the graphene sheet is shaded in gray, where $\mathbf{b}_1 = 2\pi/a(1/\sqrt{3}, 1)^T$ and $\mathbf{b}_2 = 2\pi/a(1/\sqrt{3}, -1)^T$ are the reciprocal lattice vectors. The corners of the hexagon are Dirac points, denoted \mathbf{K} and \mathbf{K}' .

²In the literature is common to find a convention where a is the carbon-carbon distance in the lattice, with value $a \approx 1.42 \text{ \AA}$. This convention adds an extra $\sqrt{3}$ term in the definition of the lattice vectors (1.2).

Here we employ a nearest-neighbor tight-binding model for the energy band in a honeycomb lattice. The Hamiltonian is given by

$$H = -t \sum_{\langle i,j \rangle} a_i^\dagger b_j + \text{h.c.}, \quad (1.4)$$

where a_i (b_j) annihilates and a_i^\dagger (b_j^\dagger) creates an electron at site \mathbf{R}_i (\mathbf{R}_j) of the sublattice A(B), and $t \approx 2.8$ eV is the nearest-neighbor hopping energy.

The energy bands of this Hamiltonian have the form [49]

$$E_s(\mathbf{k}) = st \left| 1 + e^{i\mathbf{k}\cdot\mathbf{a}_1} + e^{i\mathbf{k}\cdot\mathbf{a}_2} \right|, \quad (1.5)$$

where $s = \pm 1$ indicates the band energy. Because one carbon site has one electron on average, only the valence band $E_-(\mathbf{k})$ is completely occupied and the conduction band $E_+(\mathbf{k})$ is empty. The corresponding wavefunctions can be written as

$$\psi_s(\mathbf{k}) = \begin{pmatrix} 1 \\ -s \frac{f(\mathbf{k})}{|f(\mathbf{k})|} \end{pmatrix} \quad (1.6)$$

with $f(\mathbf{k}) \equiv |1 + e^{i\mathbf{k}\cdot\mathbf{a}_1} + e^{i\mathbf{k}\cdot\mathbf{a}_2}|$.

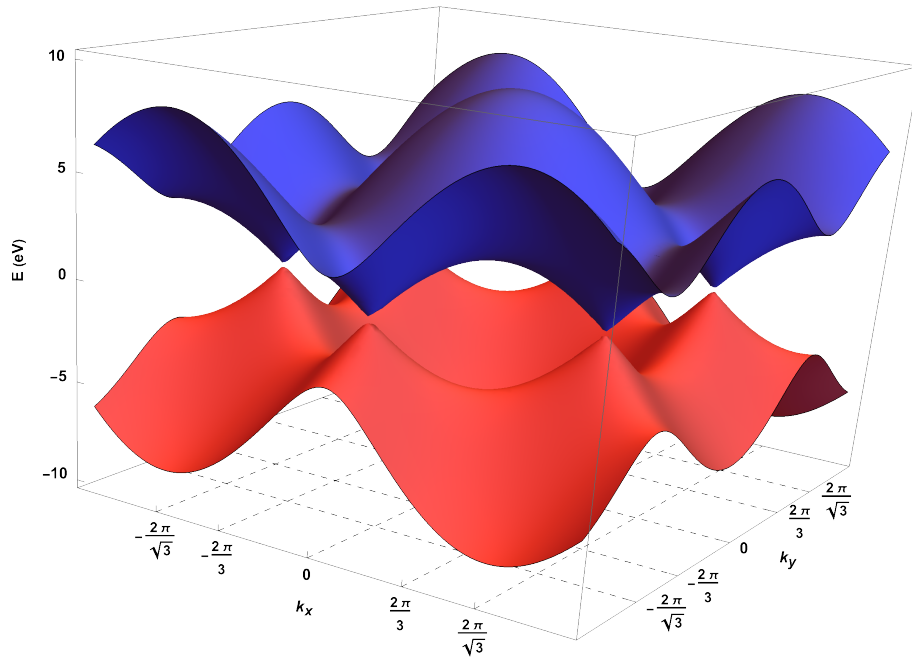


Figure 1.3: The energy dispersion variations of graphene lattice of the conduction band (blue) and valence band (red). Both bands make contact at the Dirac points \mathbf{K}, \mathbf{K}' .

Near the Γ point on Figure 1.2, both bands can be expressed as quadratic functions of $|\mathbf{k}|$,

$$E_s(\mathbf{k}) = st \left(3 - \frac{a^2 |\mathbf{k}|^2}{4} \right) + \mathcal{O}((|\mathbf{k}|a)^4), \quad (1.7)$$

where $|\mathbf{k}|a \ll 1$. At the M points, which are in the midpoints of the sides of the first Brillouin zone, the energy dispersion possesses saddle points, and the density of states diverges logarithmically.

The two bands have conical intersections (Dirac cones) at zero energy in the corners of the first Brillouin zone, see Figures 1.2 and 1.3. Near the K -points, at the corner of the first Brillouin zone, the energy dispersion is a linear function of the magnitude of the wave vector,

$$E_s(\mathbf{K} + \mathbf{q}) = sv_F |\mathbf{q}| + \mathcal{O}((|\mathbf{q}|/|\mathbf{K}|)^2) \quad (1.8)$$

where \mathbf{q} is the (pseudo)momentum measured relatively to the Dirac points with $|\mathbf{q}| \ll |\mathbf{K}|$, and, $v_F \equiv \sqrt{3}ta/2$ is the Fermi velocity in graphene, with a value $v_F \approx 10^6$ m/s. This means that electronic excitations in graphene obey a ultra-relativistic dispersion relation, but with velocity v_F .

Figure 1.3 shows six contact points between the conduction and valence bands. However, there are only two inequivalent Dirac points (also called valleys), given in (1.3), under translations generated by the reciprocal lattice vectors. Using the Fourier representation of the electron operators around \mathbf{K} or \mathbf{K}' with a slowly varying envelope momentum, these new operators satisfies a massless Dirac equation in the continuum limit. The corresponding wavefunction, called spinor or eigenspinor, has four components, with two components corresponding to each sublattice (or each valley). The details of this computation can be found in [20, 47].

1.2 Boundary Conditions

The four-component operator H takes into account contributions of two non-equivalents Dirac points (or valleys) corresponding to the \mathbf{K} and \mathbf{K}' points at the corners of the first Brillouin zone associated to the honeycomb lattice. The orthogonal sum in (1.1) is with respect to \mathbf{K} and \mathbf{K}' spaces. In many applications, the valleys do not couple, and the description is reduced to the study of the one-valley operator T only. When considering quasi-particles confined to some two-dimensional region, one could impose boundary conditions that might break the Dirac Hamiltonian's block-diagonal structure. This choice affects the energy spectrum

and its transport properties. For instance, the presence of a gap in its spectrum allows using graphene samples as semiconductor devices.

In physics literature, the so-called zigzag, armchair and infinite mass boundary conditions have attracted much attention. The first two come from the tight-binding model and they correspond to two different orientations of a straight lattice termination [4]. The zigzag boundary conditions are known to be gapless, having zero as an eigenvalue of infinite multiplicity [46], i.e., corresponding to a metallic behavior. The associated zero-energy states are well localized close to the boundary [25, 46]. Recently, Holtzmann [27] discussed the three-dimensional 4-components Dirac operator with the analogue zigzag boundary conditions. In his work, he proves that the operator is self-adjoint in L^2 for any open set, and he computes its eigenvalues in terms of the spectrum of the Dirichlet Laplacian on the domain. On the contrary, for armchair boundary conditions, the presence of a gap has been shown (see, e.g. [18, 37, 50]), and the lowest states are delocalized. Zigzag boundary conditions do not couple the valleys and thus they can be just described for T . Armchair boundary conditions mix the valleys, and it is necessary to consider the full operator H .

On the other hand, infinity mass boundary conditions do not arise from lattice termination. They were first theoretically studied in 1987 by Berry and Mondragon [16] for the two-component operator T , and experimentally studied, for instance in [40]. This case can be deduced in a continuous way starting from the zigzag boundary condition, by introducing a staggering local potential which produces confinement by an infinitely large mass term at the boundary [4, 6, 7, 48]. In the graphene description, infinite mass boundary conditions have also been used to model quantum dots or nanoribbons exhibiting a gap independent of the lattice orientation. In that way, Borrelli [17] studied this kind of boundary conditions with a potential defined by the trace of the 3D Coulomb potential, as an effective model for electron transport in graphene. The above work proves the smoothness of the solutions: infinitely many solutions exist in $C^\infty(\Omega, \mathbb{C}^2)$.

This approach has recently been the subject of intense research: for instance, in [8] it is shown that the norm resolvent of the two-components Dirac operator is convergent, as the mass m goes to infinity, for bounded and unbounded domains, and [15] includes the computation of the asymptotic expansion of the spectral quantities (eigenvalues and resolvent) with correction terms proportional to $1/m$. Moreover, in [30] the authors prove that the operator is self-adjoint for convex sectors, and it has a family of self-adjoint extensions for non-convex sectors. Recently, Cassano and Lotoreichik [19] demonstrated that there exists no self-adjoint extensions for Dirac operator with infinity mass boundary conditions in wedges, because inevitably it mixes both

valleys [31].

Furthermore, recent literature has also studied the self-adjointness of Dirac operators on domains in \mathbb{R}^3 with a mass term, also including combinations of electrostatic and Lorentz scalar δ -shell interactions for the four-spinor [10, 11, 12]. Pizichillo and Van den Bosch [38] extended this results to two-component operators on corner domains in \mathbb{R}^2 . For extensions in higher dimensions, see, for example, [34].

1.3 Definitions and Notation

We will use the convention of Kronecker product for 2×2 matrices [35]:

$$A \otimes B = \begin{pmatrix} a_{11} & a_{12} \\ a_{21} & a_{22} \end{pmatrix} \otimes B = \begin{pmatrix} a_{11}B & a_{12}B \\ a_{21}B & a_{22}B \end{pmatrix},$$

with the product property

$$(A \otimes B)(C \otimes D) = (AC) \otimes (BD).$$

Henceforth the 2×2 identity matrix and the Pauli matrices are notated as

$$\sigma_0 = \begin{pmatrix} 1 & 0 \\ 0 & 1 \end{pmatrix}, \quad \sigma_1 = \begin{pmatrix} 0 & 1 \\ 1 & 0 \end{pmatrix}, \quad \sigma_2 = \begin{pmatrix} 0 & -i \\ i & 0 \end{pmatrix}, \quad \sigma_3 = \begin{pmatrix} 1 & 0 \\ 0 & -1 \end{pmatrix}.$$

They satisfy the (anti)commutation relations

$$\begin{aligned} \{\sigma_j, \sigma_k\} &= 2\delta_{jk}, \\ [\sigma_j, \sigma_k] &= 2i\epsilon_{jkl}\sigma_l \quad \text{for } j, k, l \in \{1, 2, 3\}, \end{aligned}$$

where δ_{jk} is the Kronecker delta and ϵ_{jkl} is the Levi-Civita tensor.

Two-dimensional complex vectors on the (x, y) plane are annotated as $\mathbf{v} \equiv (v_1, v_2)^T \in \mathbb{C}^2$, and we will occasionally write $\mathbf{v}^* \equiv (v_1^*, v_2^*)^T$ as the complex conjugate vector. Otherwise, for an operator A , A^* denotes its adjoint operator and \overline{A} its complex conjugate. In particular, $\mathbf{n} = (n_1, n_2)^T$ will denote the two-dimensional outward unit normal vector to the boundary of the domain and \mathbf{t} will be the two-dimensional unit tangent vector pointing clockwise to the boundary of the domain, i.e., $\mathbf{n} \times \mathbf{t} = \hat{\mathbf{k}}$. The vectors $\hat{\mathbf{i}}, \hat{\mathbf{j}}, \hat{\mathbf{k}}$ will denote the canonical unit vectors

in \mathbb{R}^3 (or \mathbb{R}^2). Three-dimensional complex vectors are denoted with a bold font and an arrow above, $\vec{\mathbf{v}} \equiv (v_1, v_2, v_2)^T \in \mathbb{C}^3$. More specifically, the vector of the two first Pauli matrices will be $\boldsymbol{\sigma} \equiv (\sigma_1, \sigma_2)^T$ and the vector of the three Pauli matrices $\vec{\boldsymbol{\sigma}} \equiv (\sigma_1, \sigma_2, \sigma_3)^T$.

In general, a dot will denote the scalar product in \mathbb{R}^2 or \mathbb{R}^3 ,

$$\mathbf{a} \cdot \mathbf{b} = \sum_{j=1}^2 a_j b_j \quad \text{or} \quad \vec{\mathbf{a}} \cdot \vec{\mathbf{b}} = \sum_{j=1}^3 a_j b_j.$$

The \mathbb{C}^n -inner product will be denoted by $(\cdot, \cdot)_{\mathbb{C}^n}$ for $n = \{2, 4\}$. In this work, we will consider a fixed domain Ω , also $\|\cdot\|$ and (\cdot, \cdot) will be the norm and scalar product in the spaces $L^2(\Omega, \mathbb{C}^n)$ for $n = \{2, 4\}$.

We mainly study the two-valley four-component Dirac operator defined by the differential expression

$$H = \sigma_0 \otimes T = \begin{pmatrix} T & 0 \\ 0 & T \end{pmatrix},$$

acting on $L^2(\Omega, \mathbb{C}^4)$, which take into account contributions of both valleys, in units where $\hbar = v_F = 1$, and,

$$T = -i\boldsymbol{\sigma} \cdot \nabla = -i \begin{pmatrix} 0 & \partial_1 - i\partial_2 \\ \partial_1 + i\partial_2 & 0 \end{pmatrix}$$

is the two-component Dirac operator acting in one valley. When we refer to a domain of a specific operator, we will denote $\mathcal{D}(\cdot)$. Besides, we will use the abbreviations *zz*, *ac*, ∞ to refer to the zigzag, armchair and infinite mass boundary conditions, respectively.

We usually use the function B_η defined as

$$B_\eta \equiv \min \left(\left| \frac{\cos \eta}{1 - \sin \eta} \right|, \left| \frac{1 - \sin \eta}{\cos \eta} \right| \right), \quad (1.9)$$

with η a real function at the boundary of the domain.

Chapter 2

Two–valley Dirac operator with boundary conditions

The general boundary conditions are associated with a four real parameter family matrices which fixes the eigenspinors at the boundary [3, 4]. They depend on one mixing angle Λ , two three–dimensional unit vectors \vec{n}_1 and \vec{n}_2 mutually orthogonal to the normal to the boundary, and one three–dimensional unit vector $\vec{\nu}$ on the Bloch sphere of valley isospins.

In this section, we briefly discuss the one–valley description of the Dirac equation and we state the main theorems about the self–adjointness and the spectral gap in graphene quantum dots [13, 14]. Next, we discuss the appropriated boundary conditions for the two–valley Dirac operator, and we explicitly derive the structure of the local boundary matrices.

2.1 One–Valley Description

We consider the massless two–dimensional two–component Dirac operator on a bounded domain $\Omega \subset \mathbb{R}^2$ with C^2 –boundary $\partial\Omega$,

$$T \equiv -i\boldsymbol{\sigma} \cdot \boldsymbol{\nabla} = -i \begin{pmatrix} 0 & \partial_1 - i\partial_2 \\ \partial_1 + i\partial_2 & 0 \end{pmatrix}$$

acting on a subset of $\mathcal{H} = L^2(\Omega, \mathbb{C}^2)$, in appropriated units. In particular, we are interested in operators T_η acting as T on functions in the domain

$$\mathcal{D}(T_\eta) \equiv \{u \in H^1(\Omega, \mathbb{C}^2) \mid A_\eta \gamma u = \gamma u\}, \quad (2.1)$$

where γ is the trace operator on $\partial\Omega$, and A_η is defined as

$$A_\eta = (\boldsymbol{\sigma} \cdot \mathbf{t}) \cos \eta + \sigma_3 \sin \eta, \quad (2.2)$$

with \mathbf{t} the unit vector tangent to the boundary and η a real function on the boundary. The physical relevant cases of η correspond to a constant on each connected component of $\partial\Omega$. One of the most commonly used is when $\eta = 0$ or $\eta = \pi$, known as infinite mass boundary conditions. This kind of boundary conditions was first used by Berry and Mondragon to study neutrino billiards on two-dimensions [16]. Besides, the zigzag boundary conditions are given by $\eta = \pi/2$ or $\eta = 3\pi/2$.

The 2×2 matrix A_η is a unitary and hermitian matrix satisfying the anticommutation relation

$$\{A_\eta, \boldsymbol{\sigma} \cdot \mathbf{n}\} = 0. \quad (2.3)$$

This property is straightforward since the anticommutation relations of the Pauli matrices and the orthogonality between the normal and the tangent vectors. In particular, this is the only family of local boundary conditions making T into a symmetric operator on $H^1(\Omega, \mathbb{C}^2)$. Using integration by parts and the hermiticity of the Pauli matrices, we have, for all $u, v \in H^1(\Omega, \mathbb{C}^2)$,

$$\begin{aligned} \langle u, Tv \rangle &= -i \int_{\Omega} (u, (\boldsymbol{\sigma} \cdot \nabla)v)_{\mathbb{C}^2}, \\ &= -i \int_{\Omega} \nabla \cdot (u, \boldsymbol{\sigma}v)_{\mathbb{C}^2} + i \int_{\Omega} ((\boldsymbol{\sigma} \cdot \nabla)v, u)_{\mathbb{C}^2}, \\ &= \langle Tu, v \rangle - i \int_{\partial\Omega} (u, (\boldsymbol{\sigma} \cdot \mathbf{n})v)_{\mathbb{C}^2}, \end{aligned}$$

where \mathbf{n} is the outward unit normal vector to the boundary. Therefore, if $u, v \in \mathcal{D}(T_\eta)$, the boundary term, corresponding to the total quantum normal current to the boundary, cancels since the relation (2.3). The conditions when T_η is self-adjoint in a domain contained on $H^1(\Omega, \mathbb{C}^2)$ are shown in the reference [13]. We include its main theorem by completeness.

Theorem 2.1 (Theorem 1.1, [13]).

Given $\Omega \subset \mathbb{R}^2$, bounded, with C^2 -boundary, and $\eta \in C^1(\partial\Omega, \mathbb{C}^2)$, define T_η as above. If $\cos \eta(s) \neq 0$ for all $s \in \partial\Omega$, then T_η is self-adjoint on $\mathcal{D}(T_\eta)$.

In this case, the spectrum of T_η consists of eigenvalues of finite multiplicity accumulating only in $\pm\infty$ due to the compact embedding of $H^1(\Omega, \mathbb{C}^2)$ in $L^2(\Omega, \mathbb{C}^2)$ and thus, the compactness of the resolvent of T_η . On the contrary, the zigzag case ($\cos \eta = 0$), the associated operator is not self-adjoint on a domain included in $H^1(\Omega, \mathbb{C}^2)$ and 0 is an eigenvalue of infinite multiplicity. Actually, the square of the spectrum of the Dirac operator with zigzag boundary conditions coincides with the spectrum of the Dirichlet Laplacian in the domain, except at zero [25, 46]. Furthermore, if $\cos \eta(s)$ tends to zero at least quadratically at some point $s_0 \in \partial\Omega$, then 0 is in the essential spectrum of the Dirac operator. Therefore, if some part of the boundary has a zigzag termination, the domain of the self-adjoint realization of the operator cannot be included in $H^1(\Omega, \mathbb{C}^4)$ [13].

The proof of Theorem 2.1, presented in [13], uses the fact that T_η corresponds to a symmetric operator. The inclusion $\mathcal{D}(T_\eta^*) \subset \mathcal{D}(T_\eta)$ is straightforward but showing the inclusion $\mathcal{D}(T_\eta) \subset \mathcal{D}(T_\eta^*)$ is the difficult step. First, they show the regularity of the boundary values of functions in the domain of the adjoint operator. Next, they establish the desired result in the unit disc.. Finally, using the Riemann mapping theorem, they prove the general case.

Theorem 2.2 (Theorem 1, [14]).

Take $\Omega \subset \mathbb{R}^2$ simply connected with C^2 -boundary. Let η be a constant such that $\cos \eta \neq 0$ and define T_η as above. Define $B_\eta \equiv \min(|\cos \eta / (1 - \sin \eta)|, |(1 - \sin \eta) / \cos \eta|)$. If λ is an eigenvalue of T_η , then

$$\lambda^2 \geq \frac{2\pi}{|\Omega|} B_\eta^2. \quad (2.4)$$

This lower bound implies a spectral gap larger than $(8\pi)^{1/2}|\Omega|^{-1/2}B_\eta$. In physical units for infinite mass boundary conditions ($B_\eta = 1$) it gives a gap larger than $(8\pi)^{1/2}\hbar v_F|\Omega|^{-1/2}$. Therefore, to obtain a gap of 1 eV, one needs a domain with an area of about 10 nm. For $\cos \eta = 0$ the spectrum is gapless: zigzag boundary conditions. This lower bound is not sharp but is accurate with the case of a disc [16]. In that case, the lowest eigenvalue corresponds to $k_0 \approx 1.435$, and the lower bound of Theorem 2.2 reads

$$k_0 > \sqrt{2} \approx 1.414.$$

The proof of Theorem 2.2 consists in extend the result for $\eta = 0$ to the general case, based on the ideas presented in [9]. See [14] for more details.

2.2 Two-Valley Description

First, using integration by parts and the hermiticity of the Pauli matrices, we can establish the necessary boundary conditions for H to be a symmetric operator. We have, for all $u, v \in H^1(\Omega, \mathbb{C}^4)$,

$$\begin{aligned} \langle u, Hv \rangle &= -i \int_{\Omega} (u, \sigma_0 \otimes (\boldsymbol{\sigma} \cdot \nabla)v)_{\mathbb{C}^4}, \\ &= -i \int_{\Omega} \nabla \cdot (u, \sigma_0 \otimes \boldsymbol{\sigma}v)_{\mathbb{C}^4} + i \int_{\Omega} (\sigma_0 \otimes (\boldsymbol{\sigma} \cdot \nabla)v, u)_{\mathbb{C}^4}, \\ &= \langle Hu, v \rangle - i \int_{\partial\Omega} (u, \sigma_0 \otimes (\boldsymbol{\sigma} \cdot \mathbf{n})v)_{\mathbb{C}^4}, \end{aligned} \quad (2.5)$$

where \mathbf{n} is the two-dimensional outward unit normal vector to $\partial\Omega$, the boundary of Ω . Therefore, appropriated boundary conditions cancel the boundary term on the right side. If we assume that the four-spinors satisfies a relation of the type

$$u = Mu \quad \text{on} \quad \partial\Omega, \quad (2.6)$$

with a unitary and self-adjoint matrix multiplication operator $M (= M^* = M^{-1})$ acting from $L^2(\partial\Omega, \mathbb{C}^4)$ to $L^2(\partial\Omega, \mathbb{C}^4)$ that fixes the four-spinors at the boundary. Then, the requirement of absence of a current normal to the boundary, given in the second term of (2.5), holds if and only if

$$\{M, \mathbf{J} \cdot \mathbf{n}\} = \{M, \sigma_0 \otimes (\boldsymbol{\sigma} \cdot \mathbf{n})\} = 0 \quad \text{on} \quad \partial\Omega. \quad (2.7)$$

In particular, for these cases, the Dirac Hamiltonian is formally symmetric and satisfies the bag condition [16].

The general 4×4 matrices M which satisfy (2.6) and (2.7) are subclasses of the four-parameter family solution, they were obtained in [3, 4],

$$M = (\sigma_0 \otimes (\vec{\boldsymbol{\sigma}} \cdot \vec{\mathbf{n}}_1)) \sin \Lambda + ((\vec{\boldsymbol{\sigma}} \cdot \vec{\boldsymbol{\nu}}) \otimes (\vec{\boldsymbol{\sigma}} \cdot \vec{\mathbf{n}}_2)) \cos \Lambda, \quad (2.8)$$

for certain three-dimensional unit vectors $\vec{\mathbf{n}}_1, \vec{\mathbf{n}}_2, \vec{\boldsymbol{\nu}}$ such that $\vec{\mathbf{n}}_1 \cdot \vec{\boldsymbol{\nu}} = \vec{\mathbf{n}}_2 \cdot \vec{\boldsymbol{\nu}} = \vec{\mathbf{n}}_1 \cdot \vec{\mathbf{n}}_2 = 0$, a sufficiently smooth real function $\Lambda : \partial\Omega \rightarrow [0, 2\pi)$ known as the *mixing angle*, and $\vec{\boldsymbol{\sigma}} = (\sigma_1, \sigma_2, \sigma_3)^T$ the three Pauli matrices. When $\cos \Lambda \neq 0$, the function Λ plays the role of mixing the eigenspinor components of both valleys.

We will work with Dirac operators H_M acting as (1.1) on functions in the domain

$$\mathcal{D}(H_M) \equiv \mathcal{D}(H; M) = \{u \in H^1(\Omega, \mathbb{C}^4) \mid P_{M,-}\gamma u = 0\}. \quad (2.9)$$

Here γ is the trace operator on $\partial\Omega$ and the orthogonal projections $P_{M,\pm}$ are defined as

$$P_{M,\pm} = \frac{1}{2}(1 \pm M). \quad (2.10)$$

The relation (2.6) is equivalent to $P_{M,-}\gamma u = 0$. Thus, if $u, v \in \mathcal{D}(H_M)$, the boundary term in (2.5) cancels because of the relation (2.7).

Particularly, the boundary mixing matrix associated with the zigzag, armchair and infinity mass boundary conditions are

$$M_{zz} \equiv \pm(\sigma_3 \otimes \sigma_3), \quad (2.11a)$$

$$M_{ac} \equiv (\boldsymbol{\sigma} \cdot \boldsymbol{\nu}) \otimes (\boldsymbol{\sigma} \cdot \boldsymbol{t}), \quad (2.11b)$$

$$M_{\infty} \equiv \pm\sigma_3 \otimes (\boldsymbol{\sigma} \cdot \boldsymbol{t}), \quad (2.11c)$$

respectively. Where $\boldsymbol{\nu}$ is a unit vector on the (x, y) plane.

2.3 Boundary Matrix M

In this section, we show that the matrix operator M can be written as a four-parameter family given in equation (2.8). This matrix satisfies the following conditions

$$M^* = M, M^2 = 1, \text{ and}, \quad (2.12a)$$

$$\{M, \sigma_0 \otimes \boldsymbol{\sigma} \cdot \boldsymbol{n}\} = 0. \quad (2.12b)$$

First, we can express a hermitian 4×4 matrix as a linear combination of the Kronecker product between the 2×2 Pauli matrices,

$$M = \sum_{i,j=0}^3 c_{ij}(\sigma_i \otimes \sigma_j),$$

where $c_{ij} \in \mathbb{R}$ because M is self-adjoint. For $\vec{\mathbf{a}}, \vec{\mathbf{b}} \in \mathbb{R}^3$, the following properties of the Pauli matrices are useful to establish the conditions on these real coefficients c_{ij} ,

$$(\vec{\sigma} \cdot \vec{\mathbf{a}})(\vec{\sigma} \cdot \vec{\mathbf{b}}) = (\vec{\mathbf{a}} \cdot \vec{\mathbf{b}}) \sigma_0 + i \vec{\sigma} \cdot (\vec{\mathbf{a}} \times \vec{\mathbf{b}}), \quad (2.13a)$$

$$\{\sigma_j, \vec{\sigma} \cdot \vec{\mathbf{a}}\} = 2a_j \sigma_0 (1 - \delta_{j0}) + 2(\vec{\sigma} \cdot \vec{\mathbf{a}}) \delta_{j0}. \quad (2.13b)$$

Using the anticommutation relation (2.12b) and (2.13b), we obtain

$$\begin{aligned} \{M, \sigma_0 \otimes \vec{\sigma} \cdot \mathbf{n}\} &= \sum_{i,j=0}^3 c_{ij} (\sigma_i \otimes \{\sigma_j, \vec{\sigma} \cdot \mathbf{n}\}) \\ &= 2 \sum_{i=0}^3 \sigma_i \otimes \left(c_{i0} (\vec{\sigma} \cdot \mathbf{n}) + \sigma_0 \sum_{j=1}^3 c_{ij} n_j \right) = 0. \end{aligned}$$

Thus, the term in parenthesis must vanish. This condition can be rewritten as

$$c_{i0} \begin{pmatrix} 0 & n^* \\ n & 0 \end{pmatrix} + \begin{pmatrix} \vec{\mathbf{c}}_i \cdot \vec{\mathbf{n}} & 0 \\ 0 & \vec{\mathbf{c}}_i \cdot \vec{\mathbf{n}} \end{pmatrix} = 0.$$

where $n(s) = n_1(s) + i n_2(s)$ is the outward unit normal vector seen as a complex number and $\vec{\mathbf{n}} = (\mathbf{n}, 0)^T$. Since $n(s) \neq 0$, this implies $c_{i0} = 0$ and $\vec{\mathbf{c}}_i \cdot \vec{\mathbf{n}} = 0$ for all $i = \{0, 1, 2, 3\}$, with $\vec{\mathbf{c}}_i \equiv (c_{i1}, c_{i2}, c_{i3})^T$. Hence,

$$M = \sum_{i=0}^3 (\sigma_i \otimes \vec{\sigma} \cdot \vec{\mathbf{c}}_i).$$

In this notation, we have

$$M = \begin{pmatrix} \vec{\sigma} \cdot (\vec{\mathbf{c}}_0 + \vec{\mathbf{c}}_3) & \vec{\sigma} \cdot (\vec{\mathbf{c}}_1 - i\vec{\mathbf{c}}_2) \\ \vec{\sigma} \cdot (\vec{\mathbf{c}}_1 + i\vec{\mathbf{c}}_2) & \vec{\sigma} \cdot (\vec{\mathbf{c}}_0 - \vec{\mathbf{c}}_3) \end{pmatrix}.$$

Using the relation (2.13a),

$$M^2 = \begin{pmatrix} ((\vec{\mathbf{c}}_0 + \vec{\mathbf{c}}_3)^2 + \vec{\mathbf{c}}_1^2 + \vec{\mathbf{c}}_2^2) \sigma_0 + 2\vec{\sigma} \cdot (\vec{\mathbf{c}}_1 \times \vec{\mathbf{c}}_2) & 2\vec{\mathbf{c}}_0 \cdot (\vec{\mathbf{c}}_1 - i\vec{\mathbf{c}}_2) \sigma_0 + 2i\vec{\sigma} \cdot (\vec{\mathbf{c}}_3 \times (\vec{\mathbf{c}}_1 - i\vec{\mathbf{c}}_2)) \\ 2\vec{\mathbf{c}}_0 \cdot (\vec{\mathbf{c}}_1 + i\vec{\mathbf{c}}_2) \sigma_0 + 2i\vec{\sigma} \cdot (\vec{\mathbf{c}}_3 \times (\vec{\mathbf{c}}_1 + i\vec{\mathbf{c}}_2)) & ((\vec{\mathbf{c}}_0 - \vec{\mathbf{c}}_3)^2 + \vec{\mathbf{c}}_1^2 + \vec{\mathbf{c}}_2^2) \sigma_0 + 2\vec{\sigma} \cdot (\vec{\mathbf{c}}_1 \times \vec{\mathbf{c}}_2) \end{pmatrix}.$$

The condition $M^2 = 1$ implies

$$\begin{aligned}\vec{c}_0 \cdot \vec{c}_3 &= 0 \quad , \quad \vec{c}_1 \times \vec{c}_2 = \vec{0} \quad , \quad \vec{c}_0^2 + \vec{c}_3^2 + \vec{c}_1^2 + \vec{c}_2^2 = 1, \\ \vec{c}_0 \cdot \vec{c}_1 &= \vec{c}_0 \cdot \vec{c}_2 = 0 \quad , \quad \vec{c}_1 \times \vec{c}_3 = \vec{c}_2 \times \vec{c}_3 = \vec{0}.\end{aligned}$$

Therefore, \vec{c}_0 is orthogonal to $\vec{c}_1, \vec{c}_2, \vec{c}_3$. Moreover, $\vec{c}_i = c_i \vec{n}_2$ for $i = 1, 2, 3$, for some unit vector \vec{n}_2 . Finally, since the condition $\vec{c}_0^2 + \vec{c}_1^2 + \vec{c}_2^2 + \vec{c}_3^2 = 1$, it follows that

$$M = (\sigma_0 \otimes (\vec{\sigma} \cdot \vec{n}_1)) \sin \Lambda + ((\vec{\sigma} \cdot \vec{\nu}) \otimes (\vec{\sigma} \cdot \vec{n}_2)) \cos \Lambda,$$

where $\vec{\nu}, \vec{n}_1, \vec{n}_2$ are tridimensional unit vectors such that $\vec{n}_1 \cdot \vec{n}_2 = \vec{n}_1 \cdot \vec{n} = \vec{n}_2 \cdot \vec{n} = 0$ and Λ is a real function.

We compute the outer products,

$$\begin{aligned}M &= M^{(1)} \sin \Lambda + M^{(2)} \cos \Lambda, \\ \text{where } M^{(1)} &= \begin{pmatrix} \vec{\sigma} \cdot \vec{n}_1 & 0 \\ 0 & \vec{\sigma} \cdot \vec{n}_1 \end{pmatrix} \quad \text{and} \quad M^{(2)} = \begin{pmatrix} \sin \phi(\vec{\sigma} \cdot \vec{n}_2) & \nu^* \cos \phi(\vec{\sigma} \cdot \vec{n}_2) \\ \nu \cos \phi(\vec{\sigma} \cdot \vec{n}_2) & -\sin \phi(\vec{\sigma} \cdot \vec{n}_2) \end{pmatrix}.\end{aligned}\tag{2.14}$$

Here, $\nu(s) = \nu_1(s) + i\nu_2(s)$ is the orthogonal projection of $\vec{\nu}$ on the (x, y) plane seen as a complex number, and ϕ is the angle between $\vec{\nu}$ and the (x, y) plane.

We explicitly compute the dot products

$$\begin{aligned}\vec{\sigma} \cdot \vec{n}_1 &= (\vec{\sigma} \cdot \vec{t}) \cos \theta + \sigma_3 \sin \theta, \\ \vec{\sigma} \cdot \vec{n}_2 &= -(\vec{\sigma} \cdot \vec{t}) \sin \theta + \sigma_3 \cos \theta,\end{aligned}$$

with θ the angle between \vec{n}_1 and the (x, y) plane, defined such that $\vec{n}_1 \times \vec{n}_2 = \vec{n}$. This means that $\vec{n}, \vec{n}_1, \vec{n}_2$ are an orthonormal basis of \mathbb{R}^3 .

Chapter 3

Unitary Equivalence

First of all, we start with the four-parameter of matrices given by

$$M = (\sigma_0 \otimes (\vec{\sigma} \cdot \vec{n}_1)) \sin \Lambda + ((\vec{\sigma} \cdot \vec{\nu}) \otimes (\vec{\sigma} \cdot \vec{n}_2)) \cos \Lambda,$$

for certain three-dimensional unit vectors $\vec{n}_1, \vec{n}_2, \vec{\nu}$ such that $\vec{n}_1 \cdot \vec{n} = \vec{n}_2 \cdot \vec{n} = \vec{n}_1 \cdot \vec{n}_2 = 0$, a sufficiently smooth $\Lambda : \partial\Omega \rightarrow [0, 2\pi)$ known as the *mixing angle*, and $\vec{\sigma} = (\sigma_1, \sigma_2, \sigma_3)^T$ the three Pauli matrices. This family satisfies the properties

$$M^* = M, M^2 = 1, \text{ and,}$$

$$\{M, \sigma_0 \otimes \sigma \cdot \mathbf{n}\} = 0.$$

Theorem 3.1. *Let $\Omega \subset \mathbb{R}^2$, bounded, with C^2 -boundary. The boundary matrices M in (2.8), for the Dirac operator H_M in (2.9), are unitarily equivalent to the boundary matrices*

$$M(\eta_1, \eta_2) = \begin{pmatrix} A_{\eta_1} & 0 \\ 0 & A_{\eta_2} \end{pmatrix},$$

with A_η defined in (2.2). Given $\eta_1, \eta_2 \in C^1(\partial\Omega, \mathbb{R})$ such that $\cos \eta_1(s) \neq 0$ and $\cos \eta_2(s) \neq 0$ for all $s \in \partial\Omega$, H_M is self-adjoint.

Moreover, in the particular case when η_1, η_2 are constants, for any eigenvalue λ of H_M we have

$$\lambda^2 \geq \frac{2\pi}{|\Omega|} \min \{B_{\eta_1}^2, B_{\eta_2}^2\}.$$

Theorem 3.1 implies that we have two copies of the two–component operator studied previously. Actually, this means that we may focus our attention only in the spectral properties of the two–component operator defined in one of the valleys instead of study the complete operator for both valleys.

Specifically, we straightforwardly obtain that the Dirac operators with armchair boundary conditions H_{ac} , defined by M_{ac} (2.11b), and with infinity mass boundary conditions H_∞ , defined by the matrix M_∞ (2.11c), are unitarily equivalent. In consequence, the following corollary holds.

Corollary 3.2. *The spectra of H_{ac} and H_∞ coincide.*

To provide a proof of Theorem 3.1 we need to make explicit the unitary transformations block–diagonalizing the boundary matrices M in (2.8), into two copies of A_η . Consequently, we start with the following lemma.

Lemma 3.3.

The four–parameter family of matrices

$$M = (\sigma_0 \otimes (\vec{\sigma} \cdot \vec{n}_1)) \sin \Lambda + ((\vec{\sigma} \cdot \vec{\nu}) \otimes (\vec{\sigma} \cdot \vec{n}_2)) \cos \Lambda$$

are unitarily equivalent to the two–parameter family of matrices

$$M(\eta_1, \eta_2) = \begin{pmatrix} A_{\eta_1} & 0 \\ 0 & A_{\eta_2} \end{pmatrix},$$

with $A_\eta = (\boldsymbol{\sigma} \cdot \mathbf{t}) \cos \eta + \sigma_3 \sin \eta$.

We explicitly have that

$$\begin{aligned} M^{(1)} &\equiv (\sigma_0 \otimes (\vec{\sigma} \cdot \vec{n}_1)) \\ &= \sigma_0 \otimes ((\boldsymbol{\sigma} \cdot \mathbf{t}) \cos \theta + \sigma_3 \sin \theta) \\ &= \begin{pmatrix} (\boldsymbol{\sigma} \cdot \mathbf{t}) \cos \theta + \sigma_3 \sin \theta & 0 \\ 0 & (\boldsymbol{\sigma} \cdot \mathbf{t}) \cos \theta + \sigma_3 \sin \theta \end{pmatrix}, \end{aligned} \tag{3.1}$$

where \mathbf{t} is the two–dimensional unit tangent vector pointing clockwise to the boundary of the domain ($\mathbf{n} \times \mathbf{t} = \hat{\mathbf{k}}$). We write $\boldsymbol{\sigma} = (\sigma_1, \sigma_2)^T$ as the usual first two Pauli matrices. Besides,

$$\begin{aligned}
 M^{(2)} &\equiv (\vec{\sigma} \cdot \vec{\nu}) \otimes (\vec{\sigma} \cdot \vec{n}_2) \\
 &= \begin{pmatrix} \sin \phi & \nu^* \cos \phi \\ \nu \cos \phi & -\sin \phi \end{pmatrix} \otimes (-\vec{\sigma} \cdot \mathbf{t} \sin \theta + \sigma_3 \cos \theta) \\
 &= \begin{pmatrix} \sin \phi(-\vec{\sigma} \cdot \mathbf{t} \sin \theta + \sigma_3 \cos \theta) & \nu^* \cos \phi(-\vec{\sigma} \cdot \mathbf{t} \sin \theta + \sigma_3 \cos \theta) \\ \nu \cos \phi(-\vec{\sigma} \cdot \mathbf{t} \sin \theta + \sigma_3 \cos \theta) & -\sin \phi(-\vec{\sigma} \cdot \mathbf{t} \sin \theta + \sigma_3 \cos \theta) \end{pmatrix},
 \end{aligned} \tag{3.2}$$

where $\nu(s) = \nu_1(s) + i\nu_2(s)$ is the orthogonal projection at the (x, y) plane of the unit vector $\vec{\nu}$, seen as a unit complex number. Here θ and ϕ are real functions on the boundary.

3.1 Main Theorem Proof

Prior to present a proof of Theorem 3.1, we need to prove Lemma 3.3.

Proof of Lemma 3.3.

Firstly, using the unitary transformation given by the matrix

$$U_\nu \equiv \begin{pmatrix} \nu \sigma_0 & 0 \\ 0 & \sigma_0 \end{pmatrix} = \begin{pmatrix} \nu & 0 \\ 0 & 1 \end{pmatrix} \otimes \sigma_0, \tag{3.3}$$

we can restrict our attention to $\nu = 1$. This transformation leaves the Hamiltonian $H = \sigma_0 \otimes T$ and the matrix $M^{(1)}$ invariant. Contrarily, the matrix $M^{(2)}$ transforms as

$$\begin{aligned}
 U_\nu M^{(2)} U_\nu^* &= \begin{pmatrix} \nu & 0 \\ 0 & 1 \end{pmatrix} \begin{pmatrix} \sin \phi & \nu^* \cos \phi \\ \nu \cos \phi & -\sin \phi \end{pmatrix} \begin{pmatrix} \nu^* & 0 \\ 0 & 1 \end{pmatrix} \otimes (\vec{\sigma} \cdot \vec{n}_2) \\
 &= \begin{pmatrix} \nu & 0 \\ 0 & 1 \end{pmatrix} \begin{pmatrix} \nu^* \sin \phi & \nu^* \cos \phi \\ \cos \phi & -\sin \phi \end{pmatrix} \otimes (\vec{\sigma} \cdot \vec{n}_2) \\
 &= \begin{pmatrix} \sin \phi & \cos \phi \\ \cos \phi & -\sin \phi \end{pmatrix} \otimes (\vec{\sigma} \cdot \vec{n}_2).
 \end{aligned}$$

Next, for $\cos \phi \neq 0$, using the unitary transformation given by the matrix

$$U_\phi = \frac{1}{\sqrt{2}} \begin{pmatrix} \sqrt{1 + \sin \phi} & -\sqrt{1 - \sin \phi} \\ \cos \phi / \sqrt{1 + \sin \phi} & \cos \phi / \sqrt{1 - \sin \phi} \end{pmatrix} \otimes \sigma_0, \tag{3.4}$$

we can restrict our attention to the case $\phi = \pi/2$. This second transformation leaves the

Hamiltonian and the matrix $M^{(1)}$ invariant too. In fact, the matrix

$$P = \frac{1}{\sqrt{2}} \begin{pmatrix} \sqrt{1 + \sin \phi} & -\sqrt{1 - \sin \phi} \\ \cos \phi / \sqrt{1 + \sin \phi} & \cos \phi / \sqrt{1 - \sin \phi} \end{pmatrix} \text{ allows to diagonalize the matrix}$$

$$\begin{pmatrix} \sin \phi & \cos \phi \\ \cos \phi & -\sin \phi \end{pmatrix} = P \sigma_3 P^*,$$

for $\cos \phi \neq 0$. The case $\phi = \pi/2$ correspond exactly to $\sigma_3 \otimes (\vec{\sigma} \cdot \vec{n}_2)$. Otherwise, the case $\phi = 3\pi/2$ only differs on one minus sign, which could be absorbed in the definition of Λ .

Therefore, we can restrict our attention to the matrix

$$\widetilde{M}(\Lambda, \theta) \equiv (\sigma_0 \otimes (\vec{\sigma} \cdot \vec{n}_1)) \sin \Lambda + (\sigma_3 \otimes (\vec{\sigma} \cdot \vec{n}_2)) \cos \Lambda, \quad (3.5)$$

where $\vec{\sigma} \cdot \vec{n}_1 = (\boldsymbol{\sigma} \cdot \mathbf{t}) \cos \theta + \sigma_3 \sin \theta$ and $\vec{\sigma} \cdot \vec{n}_2 = -(\boldsymbol{\sigma} \cdot \mathbf{t}) \sin \theta + \sigma_3 \cos \theta$.

Then, we explicitly compute $\widetilde{M}(\Lambda, \theta)$ using the sum and difference trigonometric identities.

$$\begin{aligned} \widetilde{M}(\Lambda, \theta) &= \begin{pmatrix} (\boldsymbol{\sigma} \cdot \mathbf{t}) \cos \theta + \sigma_3 \sin \theta & 0 \\ 0 & (\boldsymbol{\sigma} \cdot \mathbf{t}) \cos \theta + \sigma_3 \sin \theta \end{pmatrix} \sin \Lambda + \\ &\quad \begin{pmatrix} -(\boldsymbol{\sigma} \cdot \mathbf{t}) \sin \theta + \sigma_3 \cos \theta & 0 \\ 0 & (\boldsymbol{\sigma} \cdot \mathbf{t}) \sin \theta - \sigma_3 \cos \theta \end{pmatrix} \cos \Lambda \\ &= \begin{pmatrix} \sigma_3 (\sin \Lambda \sin \theta + \cos \Lambda \cos \theta) & 0 \\ 0 & \sigma_3 (\sin \Lambda \sin \theta - \cos \Lambda \cos \theta) \end{pmatrix} + \\ &\quad \begin{pmatrix} (\boldsymbol{\sigma} \cdot \mathbf{t}) (\sin \Lambda \cos \theta - \cos \Lambda \sin \theta) & 0 \\ 0 & (\boldsymbol{\sigma} \cdot \mathbf{t}) (\sin \Lambda \cos \theta + \cos \Lambda \sin \theta) \end{pmatrix} \\ &= \begin{pmatrix} \sigma_3 \cos(\Lambda - \theta) & 0 \\ 0 & -\sigma_3 \cos(\Lambda + \theta) \end{pmatrix} + \begin{pmatrix} (\boldsymbol{\sigma} \cdot \mathbf{t}) \sin(\Lambda - \theta) & 0 \\ 0 & (\boldsymbol{\sigma} \cdot \mathbf{t}) \sin(\Lambda + \theta) \end{pmatrix} + \\ &\quad \begin{pmatrix} (\boldsymbol{\sigma} \cdot \mathbf{t}) \sin(\Lambda - \theta) + \sigma_3 \cos(\Lambda - \theta) & 0 \\ 0 & (\boldsymbol{\sigma} \cdot \mathbf{t}) \sin(\Lambda + \theta) - \sigma_3 \cos(\Lambda + \theta) \end{pmatrix}. \end{aligned}$$

After that, $\widetilde{M}(\Lambda, \theta)$ can be rewritten as

$$\widetilde{M}(\Lambda, \theta) = \begin{pmatrix} A_{\pi/2 - (\Lambda - \theta)} & 0 \\ 0 & A_{(\Lambda + \theta) - \pi/2} \end{pmatrix}.$$

Finally, the four-parameter boundary matrix M is unitarily equivalent to the matrix

$$M(\eta_1, \eta_2) = \begin{pmatrix} A_{\eta_1} & 0 \\ 0 & A_{\eta_2} \end{pmatrix},$$

for $\eta_1 \equiv \pi/2 - (\Lambda - \theta)$ and $\eta_2 \equiv (\Lambda + \theta) - \pi/2$. \square

Through Lemma 3.3, we accomplished to block-diagonalize the boundary conditions into two copies of the one valley operator, with different mixing angles. Now, we continue with the proof of our main theorem.

Proof of Theorem 3.1.

Since Theorem 2.1, we know that the two-component operator T_η , acting as T , with boundary conditions $u = A_\eta u$ is self-adjoint if and only if $\cos \eta(s) \neq 0$ for all $s \in \partial\Omega$. In this representation it is straightforward to show that $H_{M(\eta_1, \eta_2)}$, with boundary conditions defined by $M(\eta_1, \eta_2)$, is self-adjoint in the domain $\mathcal{D}(T_{\eta_1}) \oplus \mathcal{D}(T_{\eta_2})$ if and only if $\cos \eta_1(s) \neq 0$ and $\cos \eta_2(s) \neq 0$ for all $s \in \partial\Omega$. Through the unitary equivalence, the general operator H_M with boundary conditions defined by the matrix (2.8) is self-adjoint in its domain $\mathcal{D}(H_M)$ if and only if $\sin(\Lambda + \theta) \neq 0$ and $\sin(\Lambda - \theta) \neq 0$ at the boundary.

Next, through Theorem 2.2, for all $\phi \in \mathcal{D}(T_\eta)$ and $\cos \eta \neq 0$ holds the lower bound

$$\|T_\eta \phi\|^2 \geq \frac{2\pi}{|\Omega|} B_\eta^2 \|\phi\|^2,$$

Therefore, for all $\psi = (\psi_1, \psi_2, \psi_3, \psi_4)^T \in \mathcal{D}(H_{M(\eta_1, \eta_2)})$ holds

$$\|H_{M(\eta_1, \eta_2)} \psi\|^2 \geq \frac{2\pi}{|\Omega|} \left(B_{\eta_1}^2 \left\| \begin{pmatrix} \psi_1 \\ \psi_2 \end{pmatrix} \right\|^2 + B_{\eta_2}^2 \left\| \begin{pmatrix} \psi_3 \\ \psi_4 \end{pmatrix} \right\|^2 \right).$$

Thus, an eigenvalue of $H_{M(\eta_1, \eta_2)}$ satisfies the lower bound

$$\lambda^2 \geq \frac{2\pi}{|\Omega|} \min \{ B_{\eta_1}^2, B_{\eta_2}^2 \}.$$

Finally, an eigenvalue of the operator H_M satisfies the same lower bound because of the unitary equivalence; in other words, the isometry implies that both operators have the same spectra. \square

Proof of Corollary 3.2.

The armchair boundary conditions are defined by the matrix

$$M_{ac} = (\boldsymbol{\sigma} \cdot \boldsymbol{\nu}) \otimes (\boldsymbol{\sigma} \cdot \boldsymbol{t}),$$

corresponding to the case $\sin \Lambda = \sin \phi = \cos \theta = 0$ in (2.8). In the other way, the infinity mass boundary conditions are defined by the matrix, omitting (without loss of generality) the negative case,

$$M_{\infty} = \sigma_3 \otimes (\boldsymbol{\sigma} \cdot \boldsymbol{t}),$$

corresponding to the case $\sin \Lambda = \cos \phi = \cos \theta = 0$. In particular, the armchair case is obtained for $\Lambda = 0$, $\phi = \pi/2$, $\theta = 3\pi/2$, and, the infinity mass case is obtained for $\Lambda = 0$, $\phi = 0$, $\theta = 3\pi/2$. By way of explanation, both cases are unitarily equivalent because $M(\eta_1, \eta_2)$ only depends on Λ, θ , which are the same in both cases. Accordingly, both boundary conditions coincide in their spectra. Especially, the spectra of both operators are symmetric about zero. For the infinity mass boundary condition, this behavior was first noticed by Berry and Mondragon [16]. \square

Chapter 4

Symmetries

In this chapter, we distribute the boundary conditions according to two symmetries playing an essential role in physics: the electron–hole symmetry and the time reversal symmetry. In each case, we distinguish those which do not break the corresponding symmetry and those which break it. There exists physical interest in boundary conditions preserving the respective symmetry.

First, we define

$$\mathcal{E} = \sigma_3 \otimes \sigma_3, \quad (4.1)$$

as the operator associated with the electron–hole symmetry. The Dirac Hamiltonian (1.1) anti-commutes with \mathcal{E} , therefore, the eigenvalue equation satisfies this symmetry

$$\mathcal{E}H\psi = -H(\mathcal{E}\psi) = E(\mathcal{E}\psi).$$

The above means that

$$\mathcal{E}\psi = \begin{pmatrix} \psi_1 \\ -\psi_2 \\ -\psi_3 \\ \psi_4 \end{pmatrix}$$

is an eigenspinor of H with energy $-E$. This symmetry implies the creation of a hole in the sublattice B, i.e., the second and third components of the eigenspinor change their sign.

Second, we define

$$\mathcal{T} = -(\sigma_2 \otimes \sigma_2) \mathcal{K}, \quad (4.2)$$

as the time reversal operator in the valley isotropic representation, where \mathcal{K} is the complex conjugation operator [4]. The Dirac operator commutes with the operator \mathcal{T} . Therefore,

$$\mathcal{T}\psi = \begin{pmatrix} \psi_4^* \\ -\psi_3^* \\ -\psi_2^* \\ \psi_1^* \end{pmatrix}$$

is a eigenspinor of H with energy E too. This symmetry implies a change in the sign of the time: it reverses both spin and momentum signs.

Moreover, we define the sets

$$\mathcal{M}_{\mathcal{E}}^{\pm} \equiv \{M \in \mathbb{M}_{4 \times 4}(\mathbb{C}) \mid M \text{ satisfies (2.8) and } [M, \mathcal{E}]_{\pm} = 0\}, \quad (4.3)$$

$$\mathcal{M}_{\mathcal{T}}^{\pm} \equiv \{M \in \mathbb{M}_{4 \times 4}(\mathbb{C}) \mid M \text{ satisfies (2.8) and } [M, \mathcal{T}]_{\pm} = 0\}, \quad (4.4)$$

where $[A, B]_{\pm} = AB \mp BA$. The plus (minus) sign denotes the mixing matrices preserving (breaking) the electron–hole symmetry and time reversal symmetry, respectively. Also we will denote $\mathring{\mathcal{M}}_{\mathcal{E}}^{\pm}$ and $\mathring{\mathcal{M}}_{\mathcal{T}}^{\pm}$ as the sets (4.3) and (4.4) without including the boundary conditions unitarily equivalent to the zigzag orientation. Their deduction and explicit form are given in Appendix A.

The first distinction divides the mixing matrices into two families: those which commute with \mathcal{E} , and those which anticommute with \mathcal{E} . The aforesaid, in turn, implies four possible cases,

$$M_{\Lambda}^{\nu} = (\sigma_0 \otimes \sigma_3) \sin \Lambda + ((\boldsymbol{\sigma} \cdot \boldsymbol{\nu}) \otimes (\boldsymbol{\sigma} \cdot \mathbf{t})) \cos \Lambda, \quad (4.5)$$

$$M_{zz} = \pm(\sigma_3 \otimes \sigma_3), \quad (4.6)$$

$$M_{\Lambda'}^{\nu} = ((\boldsymbol{\sigma} \cdot \boldsymbol{\nu}) \otimes \sigma_3) \sin \Lambda' + (\sigma_0 \otimes (\boldsymbol{\sigma} \cdot \mathbf{t})) \cos \Lambda', \quad (4.7)$$

$$M_{\infty} = \pm\sigma_3 \otimes (\boldsymbol{\sigma} \cdot \mathbf{t}), \quad (4.8)$$

where \mathbf{t} is the two–dimensional unit tangent vector to the boundary of the domain; $\Lambda, \Lambda' \equiv$

$\pi/2 - \Lambda$ are real functions on the boundary and $\boldsymbol{\nu}$ is a unit vector on the (x, y) plane. The matrices of the first two cases commute with \mathcal{E} and in the last two cases, they anticommute with \mathcal{E} . The boundary conditions preserving the electron–hole symmetry include two cases of physical interest, namely $M_{zz} = \pm(\sigma_3 \otimes \sigma_3)$ and $M_{ac} = (\boldsymbol{\sigma} \cdot \boldsymbol{\nu}) \otimes (\boldsymbol{\sigma} \cdot \boldsymbol{t})$, which define the lattice terminations known as zigzag and armchair like boundary conditions, respectively. Moreover, the case defined by the matrix M_∞ is known as infinite mass boundary conditions.

On the other hand, if the mixing matrix commutes with \mathcal{T} , then the time reversal symmetry is preserved. This symmetry is broken when the mixing matrix anticommutes with \mathcal{T} . The first case implies that the mixing angle satisfies $\Lambda = \{0, \pi\}$ and the second, $\Lambda = \{\pi/2, 3\pi/2\}$.

In the second case, when the time reversal symmetry is broken, the mixing matrix is restricted to a one–parameter family,

$$M_{\mathcal{T}}^- = \sigma_0 \otimes A_\theta \quad \text{with} \quad A_\theta = (\boldsymbol{\sigma} \cdot \boldsymbol{t}) \cos \theta + \sigma_3 \sin \theta. \quad (4.9)$$

Here, θ is a real function on the boundary. Since, in our convention, the first and fourth components of the eigenspinors correspond to the sublattice A, and the second and third component to the sublattice B, it means that there is no mixing between spinor components of different K –points.

The boundary conditions which preserve the time reversal symmetry restrict M to a three–parameter family,

$$M_{\mathcal{T}}^+ = ((\boldsymbol{\sigma} \cdot \boldsymbol{\nu}) \cos \phi + \sigma_3 \sin \phi) \otimes A_{\theta'}, \quad (4.10)$$

where ϕ and $\theta' \equiv \pi/2 - \theta$ are real functions on the boundary and $\boldsymbol{\nu}$ is a two–dimensional unit vector.

Appendix A presents the complete deduction of matrices (4.5)–(4.10).

Corollary 4.1. *Let $\Omega \subset \mathbb{R}^2$, bounded, with C^2 –boundary. The mixing matrices preserving the electron–hole symmetry are given by*

$$\mathring{M}_{\mathcal{E}}^+ \equiv (\sigma_0 \otimes \sigma_3) \sin \Lambda + ((\boldsymbol{\sigma} \cdot \boldsymbol{\nu}) \otimes (\boldsymbol{\sigma} \cdot \boldsymbol{t})) \cos \Lambda, \quad (4.11)$$

with $\boldsymbol{\nu}$ a unit vector on the (x, y) plane and $\Lambda \in C^1(\partial\Omega)$ such that $\cos \Lambda(s) \neq 0$ for all $s \in \partial\Omega$. The corresponding Dirac operator is self–adjoint on the domain (2.9). Besides, if λ is an

eigenvalue of $H_{\mathcal{M}_\varepsilon^+}$, then

$$\lambda^2 \geq \frac{2\pi}{|\Omega|} B_\Lambda^2,$$

with B_Λ given in (1.9).

Proof of Corollary 4.1.

This subfamily of boundary matrices corresponds to the case $\theta = \phi = 0$ of the general case on Theorem 3.1. Both proves of the self-adjointness and the lower bound are straightforward. \square

Corollary 4.2. *Let $\Omega \subset \mathbb{R}^2$, bounded, with C^2 -boundary. The matrices breaking the electron-hole symmetry, not considering the infinity mass boundary conditions, are given by*

$$\mathring{\mathcal{M}}_\varepsilon^- \equiv ((\boldsymbol{\sigma} \cdot \boldsymbol{\nu}) \otimes \sigma_3) \sin \Lambda' + (\sigma_0 \otimes (\boldsymbol{\sigma} \cdot \mathbf{t})) \cos \Lambda', \quad (4.12)$$

with $\boldsymbol{\nu}$ a unit vector on the (x, y) plane and $\Lambda' \in C^1(\partial\Omega)$ such that $\cos \Lambda'(s) \neq 0$ for all $s \in \partial\Omega$. The corresponding Dirac operator is self-adjoint on the domain (2.9). Besides, if λ is an eigenvalue of $H_{\mathcal{M}_\varepsilon^-}$, then

$$\lambda^2 \geq \frac{2\pi}{|\Omega|} B_{\Lambda'}^2.$$

with $B_{\Lambda'}$ given in (1.9).

The Dirac operator with infinity mass boundary conditions, given by the matrix M_∞ , is self-adjoint on the domain $\mathcal{D}(T_0) \oplus \mathcal{D}(T_\pi)$, with $\mathcal{D}(T_\eta)$ defined as (2.1). In addition, the lower bound of Theorem 4.2 holds with $B = 1$.

Proof of Corollary 4.2.

This subfamily of boundary matrices corresponds to the case $\phi = 0$, $\theta = 3\pi/2$ and $\Lambda' = \Lambda - \pi/2$ of the general case on Theorem 3.1. Both proves of the self-adjointness and the lower bound are straightforward. \square

Corollary 4.3. *Let $\Omega \subset \mathbb{R}^2$, bounded, with C^2 -boundary. The mixing matrices preserving the time reversal symmetry are given by*

$$\mathring{\mathcal{M}}_\varepsilon^+ \equiv ((\boldsymbol{\sigma} \cdot \boldsymbol{\nu}) \cos \phi + \sigma_3 \sin \phi) \otimes A_{\theta'} \quad (4.13)$$

with ν a unit vector on the (x, y) plane and $\phi, \theta' \in C^1(\partial\Omega)$ such that $\cos\theta'(s) \neq 0$ for all $s \in \partial\Omega$. The corresponding Dirac operator is self-adjoint on the domain (2.9). Besides, if λ is an eigenvalue of $H_{\mathcal{M}_T^\pm}$, then

$$\lambda^2 \geq \frac{2\pi}{|\Omega|} B_{\theta'}^2.$$

with $B_{\theta'}$ given in (1.9).

Since [14, Theorem 1], it is straightforward to show the lower bound for the operator H with boundary conditions which break the time reversal symmetry. It just corresponds to two copies of the two-spinors case.

Proof of Corollary 4.3.

This subfamily of boundary matrices corresponds to the case $\Lambda = 0$ and $\theta' = \theta - \pi/2$ of the general case on Theorem 3.1. Both proves of the self-adjointness and the lower bound are straightforward. \square

In particular, we notice that the armchair and zigzag boundary conditions are the only cases preserving both symmetries. In appendix D, technical lemmas and theorems are included by completeness.

Chapter 5

Discussion and conclusions

In this work, we accomplished the block–diagonalization of the boundary conditions for the four–component continuum Dirac operator describing graphene quantum dots, through confining the four–parameter boundary matrix, defining the appropriate boundary conditions of a symmetric operator in the absence of normal quantum current at the boundary, to a two–parameter boundary matrix. In fact, we proved that the four–component Dirac operator is unitarily equivalent to two copies of the two–component Dirac operator. Our most important contribution consisted of finding the unit matrices, allowing realize those described above. Within this context, we identified the family of boundary conditions unitarily equivalent to zigzag edges, known to be gapless; moreover, we proved that the armchair boundary conditions are unitarily equivalent to the infinity mass boundary conditions.

Furthermore, we gave a proof of their self–adjointness of the continuum Dirac operator, not including the zigzag boundary conditions family, in a compact subset of the four components spinors in the Sobolev space $H^1(\Omega, \mathbb{C}^4)$. We also estimated a lower bound for the spectral gap of the electronic excitations on GQDs inversely proportional to the square root of the domain’s area depending on the mixing angles of both valleys.

Finally, we classified the boundary matrices according to whether they preserve or break the electron–hole symmetry and the time reversal symmetry. We also proved the spectral properties aforementioned for this subset of boundary conditions. It is of physical interest to know when a system conserves those symmetries, and when a symmetry breaking exists, spontaneous or not. For completeness, in Appendix B are included the two other physical symmetries widely studied: parity and charge conjugation. In addition, in Appendix C is established the cornerstone to pursue the analysis of the spectral properties found for GQDs for the nanotubes case.

As future work is expected to extend our results to graphene nanoribbons and carbon nanotubes: other kinds of graphene samples synthesized on laboratories with different physical and mathematical properties. Besides, we also await to include a magnetic field in our model to contemplate other phenomena such as spin transport and fractional quantum Hall effect.

Appendix A

Mixing Matrices for the electron–hole and time reversal symmetries

A.1 Electron–hole Symmetry

We define the operator \mathcal{E} associated with the electron–hole symmetry,

$$\mathcal{E} = \sigma_3 \otimes \sigma_3 = \begin{pmatrix} \sigma_3 & 0 \\ 0 & -\sigma_3 \end{pmatrix}. \quad (\text{A.1})$$

This symmetry is associated with a charge conjugation of the second and third components of the four–spinor. We note that the Dirac Hamiltonians (1.1) and (C.1) anticommute with \mathcal{E} and consequently, they satisfy the electron–hole symmetry. When the mixing matrix commutes with \mathcal{E} , then the symmetry is preserved. On the contrary, when the mixing matrix anticommutes with \mathcal{E} , then the symmetry is broken. These cases correspond to the families:

$$\mathcal{M}_{\mathcal{E}}^+ = \{M \in \mathbb{M}_{4 \times 4}(\mathbb{C}) \mid M \text{ satisfies (2.8) and } [M, \mathcal{E}] = 0\}, \quad (\text{A.2})$$

$$\mathcal{M}_{\mathcal{E}}^- = \{M \in \mathbb{M}_{4 \times 4}(\mathbb{C}) \mid M \text{ satisfies (2.8) and } \{M, \mathcal{E}\} = 0\}, \quad (\text{A.3})$$

respectively. Prior to state those matrix subsets, we need to establish some (anti)commutation relations due to the Pauli matrices properties.

For a three–dimensional unit vector $\vec{\mathbf{a}} = (a_1, a_2, a_3)^T$ holds that

$$[\vec{\boldsymbol{\sigma}} \cdot \vec{\mathbf{a}}, \sigma_3] = a_1[\sigma_1, \sigma_3] + a_2[\sigma_2, \sigma_3] + a_3[\sigma_3, \sigma_3] = -2i(-a_2\sigma_1 + a_1\sigma_2).$$

We can also define the two–dimensional unit vector $\mathbf{t}_a = -a_2\hat{\mathbf{i}} + a_1\hat{\mathbf{j}}$, corresponding to the clockwise orthogonal vector to the orthogonal projection of $\vec{\mathbf{a}}$ on the plane. Thus, the following commutation property holds,

$$[\vec{\boldsymbol{\sigma}} \cdot \vec{\mathbf{a}}, \sigma_3] = -2i(\boldsymbol{\sigma} \cdot \mathbf{t}_a). \quad (\text{A.4})$$

Similarly, since the anticommutation relation of the Pauli matrices, it follows

$$\{\vec{\boldsymbol{\sigma}} \cdot \vec{\mathbf{a}}, \sigma_3\} = 2a_3\sigma_0. \quad (\text{A.5})$$

Symmetry Preservation

Firstly, we compute separately the commutators between \mathcal{E} with $M^{(1)}$ and $M^{(2)}$, given in (2.14).

$$\begin{aligned} [M^{(1)}, E] &= \begin{pmatrix} \vec{\boldsymbol{\sigma}} \cdot \vec{\mathbf{n}}_1 & 0 \\ 0 & \vec{\boldsymbol{\sigma}} \cdot \vec{\mathbf{n}}_1 \end{pmatrix} \begin{pmatrix} \sigma_3 & 0 \\ 0 & -\sigma_3 \end{pmatrix} - \begin{pmatrix} \sigma_3 & 0 \\ 0 & -\sigma_3 \end{pmatrix} \begin{pmatrix} \vec{\boldsymbol{\sigma}} \cdot \vec{\mathbf{n}}_1 & 0 \\ 0 & \vec{\boldsymbol{\sigma}} \cdot \vec{\mathbf{n}}_1 \end{pmatrix}, \\ &= \begin{pmatrix} [\mathbf{n}_1 \cdot \boldsymbol{\sigma}, \sigma_3] & 0 \\ 0 & -[\vec{\boldsymbol{\sigma}} \cdot \vec{\mathbf{n}}_1, \sigma_3] \end{pmatrix} = \sigma_3 \otimes [\vec{\boldsymbol{\sigma}} \cdot \vec{\mathbf{n}}_1, \sigma_3], \\ [M^{(2)}, E] &= \left[\begin{pmatrix} \sin \phi(\vec{\boldsymbol{\sigma}} \cdot \vec{\mathbf{n}}_2) & \nu^* \cos \phi(\vec{\boldsymbol{\sigma}} \cdot \vec{\mathbf{n}}_2) \\ \nu \cos \phi(\vec{\boldsymbol{\sigma}} \cdot \vec{\mathbf{n}}_2) & -\sin \phi(\vec{\boldsymbol{\sigma}} \cdot \vec{\mathbf{n}}_2) \end{pmatrix}, \begin{pmatrix} \sigma_3 & 0 \\ 0 & -\sigma_3 \end{pmatrix} \right] \\ &= \begin{pmatrix} \sin \phi[\vec{\boldsymbol{\sigma}} \cdot \vec{\mathbf{n}}_2, \sigma_3] & -\nu^* \cos \phi\{\vec{\boldsymbol{\sigma}} \cdot \vec{\mathbf{n}}_2, \sigma_3\} \\ \nu \cos \phi\{\vec{\boldsymbol{\sigma}} \cdot \vec{\mathbf{n}}_2, \sigma_3\} & \sin \phi[\vec{\boldsymbol{\sigma}} \cdot \vec{\mathbf{n}}_2, \sigma_3] \end{pmatrix}, \end{aligned}$$

where $\vec{\boldsymbol{\nu}} = (\nu_1 \cos \phi, \nu_2 \cos \phi, \sin \phi)^T$ and $\nu \equiv \nu_1 + i\nu_2$ is a unit complex number.

Using (A.4) and (A.5), we obtain

$$[M^{(1)}, E] = -2i \begin{pmatrix} \boldsymbol{\sigma} \cdot \mathbf{t}_1 & 0 \\ 0 & -\boldsymbol{\sigma} \cdot \mathbf{t}_1 \end{pmatrix} = -2i\sigma_3 \otimes (\boldsymbol{\sigma} \cdot \mathbf{t}_1), \quad (\text{A.6})$$

$$[M^{(2)}, E] = 2 \begin{pmatrix} -i \sin \phi (\boldsymbol{\sigma} \cdot \mathbf{t}_2) & -\nu^* \cos \phi n_{2z} \sigma_0 \\ \nu \cos \phi n_{2z} \sigma_0 & -i \sin \phi (\boldsymbol{\sigma} \cdot \mathbf{t}_2) \end{pmatrix}. \quad (\text{A.7})$$

where $\mathbf{t}_1, \mathbf{t}_2$ are the corresponding clockwise orthonormal vectors to the orthogonal projections of $\vec{\mathbf{n}}_1, \vec{\mathbf{n}}_2$ on the (x, y) plane.

Consequently, the following equation holds

$$-i \begin{pmatrix} \boldsymbol{\sigma} \cdot \mathbf{t}_1 & 0 \\ 0 & -\boldsymbol{\sigma} \cdot \mathbf{t}_1 \end{pmatrix} \sin \Lambda + \begin{pmatrix} -i \sin \phi (\boldsymbol{\sigma} \cdot \mathbf{t}_2) & -\nu^* \cos \phi n_{2z} \sigma_0 \\ \nu \cos \phi n_{2z} \sigma_0 & -i \sin \phi (\boldsymbol{\sigma} \cdot \mathbf{t}_2) \end{pmatrix} \cos \Lambda = 0.$$

By the second term, we obtain that $\cos \phi n_{2z} \cos \Lambda = 0$. So there are 2 different possibilities.

(i) $n_{2z} = 0$.

Therefore, $\vec{\mathbf{n}}_2$ lives on the (x, y) plane, i.e., it coincides with the unit tangent \mathbf{t} , and $\vec{\mathbf{n}}_1 = \pm \hat{\mathbf{k}}$. Also,

$$\sin \phi (\boldsymbol{\sigma} \cdot \mathbf{t}_2) \cos \Lambda = 0.$$

Consequently, we have $\sin \phi = 0$. Obtaining the family (4.5):

$$M'_\Lambda = (\sigma_0 \otimes \sigma_3) \sin \Lambda + ((\boldsymbol{\sigma} \cdot \boldsymbol{\nu}) \otimes (\boldsymbol{\sigma} \cdot \mathbf{t})) \cos \Lambda. \quad (\text{A.8})$$

Here, all vectors are unitary and on the (x, y) plane.

(ii) $\cos \phi = 0$.

Therefore, $\vec{\mathbf{v}} = \pm \hat{\mathbf{k}}$. Moreover,

$$(\boldsymbol{\sigma} \cdot \mathbf{t}_1) \sin \Lambda = (\boldsymbol{\sigma} \cdot \mathbf{t}_2) \cos \Lambda = 0.$$

Consequently, the only case that is not contained above corresponds to $\sin \Lambda = 0$, $\vec{\mathbf{n}}_2 = \pm \hat{\mathbf{k}}$,

and \vec{n}_1 coincides with the unit tangent. Obtaining the zigzag boundary conditions (4.6)

$$M_{zz} = \pm(\sigma_3 \otimes \sigma_3).$$

Remark. The case $M_{ac} = (\boldsymbol{\sigma} \cdot \boldsymbol{\nu}) \otimes (\boldsymbol{\sigma} \cdot \boldsymbol{t})$, M'_Λ with $\sin \Lambda = 0$, defines the armchair boundary conditions.

Symmetry Breaking

First, we compute the anticommutators of the operator \mathcal{E} with $M^{(1)}$ and $M^{(2)}$, respectively.

$$\begin{aligned} \{M^{(1)}, E\} &= \begin{pmatrix} \{\vec{\boldsymbol{\sigma}} \cdot \vec{\boldsymbol{n}}_1, \sigma_3\} & 0 \\ 0 & -\{\vec{\boldsymbol{\sigma}} \cdot \vec{\boldsymbol{n}}_1, \sigma_3\} \end{pmatrix} = 2 \begin{pmatrix} n_{1z} \sigma_0 & 0 \\ 0 & -n_{1z} \sigma_0 \end{pmatrix}, \\ \{M^{(2)}, E\} &= \begin{pmatrix} \sin \phi \{\vec{\boldsymbol{\sigma}} \cdot \vec{\boldsymbol{n}}_2, \sigma_3\} & -\nu^* \cos \phi \{\vec{\boldsymbol{\sigma}} \cdot \vec{\boldsymbol{n}}_2, \sigma_3\} \\ \nu \cos \phi \{\vec{\boldsymbol{\sigma}} \cdot \vec{\boldsymbol{n}}_2, \sigma_3\} & \sin \phi \{\vec{\boldsymbol{\sigma}} \cdot \vec{\boldsymbol{n}}_2, \sigma_3\} \end{pmatrix} = 2 \begin{pmatrix} \sin \phi n_{2z} \sigma_0 & i\nu^* \cos \phi (\boldsymbol{\sigma} \cdot \boldsymbol{t}_2) \\ -i\nu \cos \phi (\boldsymbol{\sigma} \cdot \boldsymbol{t}_2) & \sin \phi n_{2z} \sigma_0 \end{pmatrix}. \end{aligned}$$

Finally, following the same steps above, we obtain two possible cases: $n_{2z} = 0$, $\vec{n}_1 = \pm \hat{\boldsymbol{k}}$ or $\sin \Lambda = 0$, $\vec{n}_2 = \pm \hat{\boldsymbol{k}}$. Resulting in the classes of matrices (4.7) and (4.8),

$$M'_{\Lambda'} = (\sigma_0 \otimes (\boldsymbol{\sigma} \cdot \boldsymbol{t})) \cos \Lambda' + ((\boldsymbol{\sigma} \cdot \boldsymbol{\nu}) \otimes \sigma_3) \sin \Lambda', \quad (\text{A.9})$$

$$M_\infty = \pm \sigma_3 \otimes (\boldsymbol{\sigma} \cdot \boldsymbol{t}), \quad (\text{A.10})$$

where $\boldsymbol{\nu} \in \mathbb{R}^2$ is a unit vector, \boldsymbol{t} is the unit tangent vector and $\Lambda' \equiv \pi/2 - \Lambda$.

Remark. M_∞ is associated with the infinite mass boundary conditions.

A.2 Time Reversal Symmetry

In 1987, Berry and Mondragon analyzed the two-component Dirac operator for neutrino billiards, in particular, for the so-called Africa shape [16]. Based on the work of Porter [42] and Sakurai [45], they studied discrete symmetries; such as time reversal symmetry conservation, for the Dirac equation with a four-scalar potential $V(\boldsymbol{r})$,

$$(\boldsymbol{\sigma} \cdot \boldsymbol{p} + V(\boldsymbol{r})\sigma_3)\Psi = E\Psi. \quad (\text{A.11})$$

For two–component spinors, they define an antiunitary operator \mathcal{A} with the form

$$\mathcal{A} = \mathcal{U}\mathcal{K},$$

where \mathcal{U} is unitary and \mathcal{K} represents charge conjugation. States Ψ transform as

$$\Psi' = \mathcal{A}\Psi = \mathcal{U}\mathcal{K} \begin{pmatrix} \Psi_1 \\ \Psi_2 \end{pmatrix} = \mathcal{U} \begin{pmatrix} \Psi_1^* \\ \Psi_2^* \end{pmatrix},$$

and operators \mathcal{B} transform as

$$\mathcal{B}' = \mathcal{A}\mathcal{B}\mathcal{A}^{-1} = \mathcal{U}\mathcal{K}\mathcal{B}\mathcal{K}\mathcal{U}^* = \mathcal{U}\overline{\mathcal{B}}\mathcal{U}^*. \quad (\text{A.12})$$

In particular, discrete symmetries, as the T–symmetry, are described by antiunitary operators. The operator describing time reversal symmetry for two–component spinors is given by

$$\mathcal{T}_2 \equiv i\sigma_2\mathcal{K} = \begin{pmatrix} 0 & 1 \\ -1 & 0 \end{pmatrix} \mathcal{K}.$$

This transformation reverses both momentum and spin, as well as the first term of the Dirac operator (A.11). If we include an electrical potential, there is not a sign change. Nonetheless, the sign of $V(\mathbf{r})$ is reversed because of the anticommutation relation of the Pauli matrices. Thus, the presence of a four–scalar potential breaks the the time reversal symmetry.

Following the same outline for four–component spinors, the time reversal operator in the valley isotropic representation is given by

$$\mathcal{T} = -(\sigma_2 \otimes \sigma_2) \mathcal{K} = \begin{pmatrix} 0 & 0 & 0 & 1 \\ 0 & 0 & -1 & 0 \\ 0 & -1 & 0 & 0 \\ 1 & 0 & 0 & 0 \end{pmatrix} \mathcal{K}, \quad (\text{A.13})$$

where \mathcal{K} is the complex conjugation operator [4]. It is easy to show that this transformation also reverses both momentum and spin. The eigenvalue equation of the Dirac Hamiltonian (1.1) clearly satisfies this symmetry. Besides, a four–scalar potential $V(\mathbf{r})(\sigma_3 \otimes \sigma_3)$ does not break T–symmetry for four–component spinors. The same happens if we include an electrical potential.

If M commutes with \mathcal{T} , then the T-symmetry is preserved. The T-symmetry is broken when M anticommutes with \mathcal{T} . The first case implies that the mixing angle satisfies $\Lambda = \{0, \pi\}$, and the second, $\Lambda = \{\pi/2, 3\pi/2\}$. The explicit computations are below.

Firstly, we compute the anticommutator between $M^{(1)}$ and \mathcal{T} ,

$$\begin{aligned}
\{M^{(1)}, \mathcal{T}\} &= -\{\sigma_0 \otimes \vec{\sigma} \cdot \vec{\mathbf{n}}_1, (\sigma_2 \otimes \sigma_2)\mathcal{K}\}, \\
&= -\sigma_2 \otimes \{\vec{\sigma} \cdot \vec{\mathbf{n}}_1, \sigma_2 \mathcal{K}\}, \\
&= -\sigma_2 \otimes ((\vec{\sigma} \cdot \vec{\mathbf{n}}_1)\sigma_2 + \sigma_2(\vec{\sigma}^* \cdot \vec{\mathbf{n}}_1))\mathcal{K}, \\
&= 0.
\end{aligned}$$

In the last step, we used the anticommutation relation of the Pauli matrices. Thus, the symmetry is broken when $\cos \Lambda = 0$. Next, we compute the commutator between $M^{(2)}$ and \mathcal{T} ,

$$\begin{aligned}
[M^{(2)}, \mathcal{T}] &= -[\vec{\nu} \cdot \vec{\sigma} \otimes \vec{\mathbf{n}}_2 \cdot \vec{\sigma}, (\sigma_2 \otimes \sigma_2)\mathcal{K}], \\
&= -(\vec{\nu} \cdot \vec{\sigma})\sigma_2 \otimes (\vec{\mathbf{n}}_2 \cdot \vec{\sigma})\sigma_2 \mathcal{K} + \sigma_2(\vec{\nu} \cdot \vec{\sigma}^*) \otimes \sigma_2(\vec{\mathbf{n}}_2 \cdot \vec{\sigma}^*)\mathcal{K}, \\
&= 0.
\end{aligned}$$

Again, we used the anticommutation relation of the Pauli matrices in the last step. The symmetry is preserved only if $\sin \Lambda = 0$.

Appendix B

Parity and Charge Conjugation Symmetries

In this appendix, we include two other discrete symmetries: parity and charge conjugation. Both symmetries together with the time reversal symmetry constitute the so-called CPT-symmetry. The CPT theorem establishes that the CPT symmetry holds for all physical phenomena, or more precisely, that any Lorentz invariant local quantum field theory with a hermitian Hamiltonian must have CPT symmetry.

B.1 Parity

The operator associated to parity symmetry is defined by

$$\mathcal{P} \equiv \sigma_1 \otimes \sigma_3 = \begin{pmatrix} 0 & 0 & 1 & 0 \\ 0 & 0 & 0 & -1 \\ 1 & 0 & 0 & 0 \\ 0 & -1 & 0 & 0 \end{pmatrix}.$$

Therefore, the Hamiltonian (1.1) transforms as

$$H' = \mathcal{P}H\mathcal{P}^* = -H. \tag{B.1}$$

It corresponds to a flip in the (pseudo) momentum $\mathbf{p} \rightarrow -\mathbf{p}$, through the transformation $\sigma_1 \rightarrow -\sigma_1, \sigma_2 \rightarrow -\sigma_2, \sigma_3 \rightarrow \sigma_3$. The wavefunction transforms as

$$\psi' \equiv \mathcal{P}\psi = \left(\psi_3, -\psi_4, \psi_1, -\psi_2 \right)^T. \quad (\text{B.2})$$

In presence of parity, the boundary conditions restrict mixing matrices (2.8) to commute with \mathcal{P} . We have two families,

$$M_1 = (\sigma_0 \otimes \sigma_3) \sin \Lambda + ((\boldsymbol{\sigma} \cdot \vec{\nu}_{(y,z)}) \otimes (\boldsymbol{\sigma} \cdot \mathbf{t})) \cos \Lambda, \quad (\text{B.3})$$

$$M_2 = \pm \sigma_1 \otimes \sigma_3. \quad (\text{B.4})$$

Here $\vec{\nu}_{(y,z)}$ is a unit vector in the (y, z) plane. The first family includes the infinity mass boundary conditions. The second case is not self-adjoint due to it corresponds to a rotation of the zigzag boundary conditions.

The proof of the self-adjointness is straightforward for the case $\vec{\nu}_{(y,z)} = \hat{\mathbf{k}}$. In that case, the domain of the operator is $\mathcal{D}(T_\Lambda) \oplus \mathcal{D}(T_{-\Lambda})$. The case $\vec{\nu}_{(y,z)} \neq \hat{\mathbf{k}}$ can be transformed to the case $\vec{\nu}_{(y,z)} = \hat{\mathbf{k}}$ through the unitary transformation defined by the matrix

$$U = \frac{1}{\sqrt{2 - 2 \sin \phi}} \begin{pmatrix} \cos \phi & i(\sin \phi - 1) \\ i(\sin \phi - 1) & \cos \phi \end{pmatrix} \otimes \sigma_0. \quad (\text{B.5})$$

Due to the Dirac Hamiltonian is invariant under this transformation, the final steps of the self-adjointness of the corresponding operator are analogous to that described in Chapter 3. Otherwise, the mixing matrices that anticommute with \mathcal{P} , breaking the P-symmetry, are given by

$$M_3 = (\sigma_0 \otimes (\boldsymbol{\sigma} \cdot \mathbf{t})) \sin \Lambda + ((\boldsymbol{\sigma} \cdot \vec{\nu}_{(y,z)}) \otimes \sigma_3) \cos \Lambda, \quad (\text{B.6})$$

$$M_4 = \pm \sigma_1 \otimes (\boldsymbol{\sigma} \cdot \mathbf{t}). \quad (\text{B.7})$$

It is straightforward to shown that the Dirac Hamiltonian associated to the boundary conditions defined by M_3 is self-adjoint in the domain $\mathcal{D}(T_{\pi/2-\Lambda}) \oplus \mathcal{D}(T_{\Lambda-\pi/2})$ for $\sin \Lambda \neq 0$ at the boundary. In particular, they satisfy the desired lower bound for the spectral gap. On the other hand, M_4 is a rotation of the infinity mass boundary condition; thus, it is self-adjoint in its domain and it holds Theorem 3.1 for $B = 1$.

B.2 Charge Conjugation

Charge parity corresponds to an inversion of the electrical charge of the particle, i.e., $e \rightarrow -e$. This symmetry switches all particles with their corresponding antiparticles. For two-component spinors, the antiunitary operator is given by [16]

$$\mathcal{C}_2 \equiv \sigma_1 \mathcal{K}.$$

The C-symmetry reverses momentum and energy, but no spin. The sign of a 4-scalar potential is also reversed.

For four-spinors, the corresponding operator associated to this symmetry is defined by

$$\mathcal{C} = i(\sigma_1 \otimes \sigma_1) \mathcal{K} = \begin{pmatrix} 0 & 0 & 0 & i \\ 0 & 0 & i & 0 \\ 0 & i & 0 & 0 \\ i & 0 & 0 & 0 \end{pmatrix} \mathcal{K}, \quad (\text{B.8})$$

where \mathcal{K} is the complex conjugation operator.

The Hamiltonian (1.1) transform as

$$H' = \mathcal{C} H \mathcal{C}^* = -H, \quad (\text{B.9})$$

and, four-spinors transforms as

$$\psi' = \mathcal{C} \psi = \left(i\psi_4^*, i\psi_3^*, i\psi_2^*, i\psi_1^* \right)^T. \quad (\text{B.10})$$

In presence of a non-zero magnetic field, the Dirac Hamiltonian corresponds to $\boldsymbol{\sigma} \cdot (\mathbf{p} + e\mathbf{A})$. This eigenvalue equation preserves charge conjugation symmetry for eigenspinors ψ' defined in (B.10) with energy $-E$. Thus, the minimal coupling term transforms as $\mathbf{p} + e\mathbf{A} \rightarrow -(\mathbf{p} + e\mathbf{A})$.

In presences of charge conjugation symmetry, the boundary conditions restrict mixing matrices (2.8) to commute with \mathcal{C} . We have two families,

$$M_5 = (\sigma_0 \otimes (\boldsymbol{\sigma} \cdot \mathbf{t})) \sin \Lambda + (\sigma_3 \otimes \sigma_3) \cos \Lambda, \quad (\text{B.11})$$

$$M_{ac} = (\boldsymbol{\sigma} \cdot \boldsymbol{\nu}) \otimes (\boldsymbol{\sigma} \cdot \mathbf{t}). \quad (\text{B.12})$$

The first family includes the zigzag boundary conditions, and the second corresponds to the armchair boundary conditions. M_5 is a particular case of M_3 for $\vec{\nu}_{(y,z)} = \hat{\mathbf{k}}$.

The mixing matrices (2.8) anticommuting with \mathcal{C} break the charge conjugation symmetry. We have two families,

$$M_6 = (\sigma_0 \otimes \sigma_3) \sin \Lambda + (\sigma_3 \otimes (\boldsymbol{\sigma} \cdot \mathbf{t})) \cos \Lambda, \quad (\text{B.13})$$

$$M_7 = (\boldsymbol{\sigma} \cdot \boldsymbol{\nu}) \otimes \sigma_3 \quad (\text{B.14})$$

The first includes the infinity mass boundary conditions case and it is a particular case of M_1 for $\vec{\nu}_{(y,z)} = \hat{\mathbf{k}}$. The Dirac operator with boundary conditions defined by M_7 is not self-adjoint because of it corresponds to a rotation of the zigzag boundary conditions.

Appendix C

Symmetries on Carbon Nanotubes

The structure of carbon nanotubes (CNTs), also called single-walled carbon nanotubes (SWCNTs), has been explored using high-resolution transmission electron microscopy techniques, yielding direct confirmation that CNTs are seamless cylinders derived from the honeycomb lattice representing a single atomic layer of a graphene sheet. Their diameter varies from 0.6 to about 3 nm [22]. The geometry of CNTs is defined by the chiral angle η , which corresponds to the angle between the lattice vector and the zigzag direction of the honeycomb lattice.

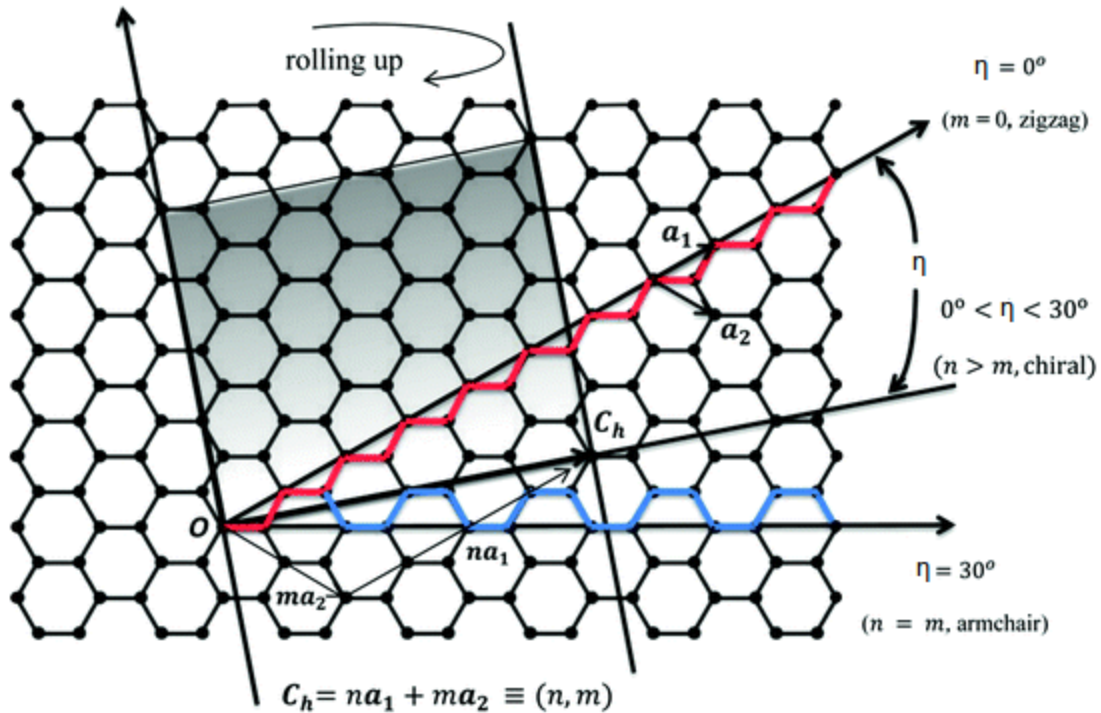


Figure C.1: Schematic of a graphene sheet and definition of geometrical parameters for describing a CNT. Image of [28].

The structure of CNTs is described by the chiral vector \mathbf{C}_h , also known as circumference vector, which represents the full circumference of the tube

$$\mathbf{C}_h = n\mathbf{a}_1 + m\mathbf{a}_2,$$

where $\mathbf{a}_1, \mathbf{a}_2$ are the lattice vectors given in equation (1.2), and n, m are two integers defining the carbon nanotube indices (n, m) [43, 44]. Furthermore, we can define the translation vector \mathbf{T}_h , also known as the propagation vector, representing the periodicity of the CNT along the tube axis. It can be obtained using that this vector is orthogonal to \mathbf{C}_h , see [23, 33]. With those two vectors, we have completely determined the structure of the CNT unit cell (shaded in Figure C.1) and thus, the full nanotube as well. In figure C.1, the so-called chiral angle η is defined as the angle between \mathbf{C}_h and \mathbf{a}_1 . If either $n = 0$ or $m = 0$, the chiral angle is 0° and there exists a zigzag structure. If $n = m$, the chiral angle is 30° and there exists an armchair structure. All other cases show chiral angles between 0° and 30° .

In particular, we can identify the diameter of the nanotube as

$$d_t \equiv \frac{|\mathbf{C}_h|}{\pi} = \frac{a\sqrt{n^2 + m^2 + nm}}{\pi}.$$

It is known that carbon nanotubes are metallic for certain chiral angles, it means that there is no gap energy around zero [29, 44]. Those cases correspond when $2n + m$ is multiple of 3, see, e.g. [5] for a complete explanation. All armchair structures are metallic and two-third of the other kind of structures too. The remaining cases are semiconductive, and they could be used to design semiconductor devices [41].

Within the context of spectral theory, the resulting Dirac Hamiltonian associated with the nanotubes [32] is given by

$$H' = \sigma_3 \otimes (\boldsymbol{\sigma}_\eta \cdot \mathbf{p}) = -i \begin{pmatrix} \boldsymbol{\sigma}_\eta \cdot \boldsymbol{\nabla} & 0 \\ 0 & -\boldsymbol{\sigma}_\eta \cdot \boldsymbol{\nabla} \end{pmatrix}, \quad (\text{C.1})$$

which results as a unitary transformation $H' = UHU^*$ of the honeycomb lattice Dirac Hamiltonian (1.1). Here, the unitary matrix U is given by $U = U_\eta U'$, with

$$U_\eta \equiv e^{i\eta\sigma_3/2} \otimes e^{i\eta\sigma_3/2} = \begin{pmatrix} e^{i\eta} & 0 & 0 & 0 \\ 0 & 1 & 0 & 0 \\ 0 & 0 & 1 & 0 \\ 0 & 0 & 0 & e^{-i\eta} \end{pmatrix}, \quad (\text{C.2})$$

$$U' \equiv \frac{1}{2}(\sigma_0 + \sigma_3) \otimes \sigma_0 + \frac{1}{2}(\sigma_0 - \sigma_3) \otimes \sigma_3 = \begin{pmatrix} \sigma_0 & 0 \\ 0 & \sigma_3 \end{pmatrix}, \quad (\text{C.3})$$

and σ_η are the first two Pauli rotated by the chiral angle η of the tube,

$$\sigma_\eta \equiv e^{i\eta\sigma_3/2}(\sigma_1, \sigma_2)e^{-i\eta\sigma_3/2}. \quad (\text{C.4})$$

Moreover, we have that spinors ψ and its respective boundary matrix M transform as

$$\psi' \equiv U\psi \quad \text{and} \quad N \equiv UMU^*.$$

Thus, an eigenspinor of H' is given by

$$\psi' \equiv (\psi'_1, \psi'_2, \psi'_3, \psi'_4)^T = (e^{i\eta}\psi_1, \psi_2, \psi_3, -e^{-i\eta}\psi_4)^T,$$

and, the 4×4 boundary matrices are given by

$$N = (\sigma_0 \otimes \vec{\sigma}_\eta \cdot \vec{n}'_1) \sin \theta + (\sigma_3 \otimes \vec{\sigma}_\eta \cdot \vec{n}'_2) \cos \theta + (\sigma_\eta \cdot \nu'_1 \otimes \sigma_0) \cos \theta + (\sigma_\eta \cdot \nu'_2 \otimes \sigma_\eta \cdot \mathbf{n}) \sin \theta, \quad (\text{C.5})$$

where \vec{n}'_1, \vec{n}'_2 are three-dimensional vectors such that $\vec{n}'_1 \perp \vec{n}'_2 \perp \vec{n}$ and $|\vec{n}'_1| = |\vec{n}'_2|$; ν'_1, ν'_2 are two-dimensional vectors such that $|\nu'_1| = |\nu'_2|$; and $|\vec{n}'_1|^2 + |\nu'_1|^2 = 1$. In terms of the parameters defined on Chapter 2, we have

$$\begin{aligned} \vec{n}'_1 &= (\mathbf{t} \sin \phi \cos \Lambda, \sin \Lambda)^T, & \nu'_1 &= \nu \cos \phi \cos \Lambda, \\ \vec{n}'_2 &= (\mathbf{t} \sin \Lambda, -\sin \phi \cos \Lambda)^T, & \nu'_2 &= \nu' \cos \phi \cos \Lambda, \end{aligned}$$

with ν' the (clockwise) orthonormal vector to ν . The family matrices presented in [32] are a subset of (C.5). Since the geometry of the CNTs, the outward unit normal to the boundary \vec{n} is completely determined by the chiral angle. Besides, it is straightforward to notice from Figure

C.1 that

$$\vec{n} = (\sin \eta, \cos \eta, 0)^T. \quad (\text{C.6})$$

In the same way, an operator \mathcal{A} , defining a certain symmetry, transforms as

$$\mathcal{A}' = U\mathcal{A}U^*. \quad (\text{C.7})$$

We continue this appendix with the relevant physical symmetries in carbon nanotubes.

C.1 Electron–Hole Symmetry

The operator defining this symmetry, $\mathcal{E} = \sigma_3 \otimes \sigma_3$, transforms as

$$\mathcal{E}' = U\mathcal{E}U^* = \sigma_0 \otimes \sigma_3. \quad (\text{C.8})$$

Since the matrix U satisfies the commutation relation $[\mathcal{E}, U] = 0$, the eigenvalue equation for H' satisfies electron–hole symmetry for the eigenspinor

$$\tilde{\psi} = \mathcal{E}'\psi' = (\psi'_1, \psi'_2, \psi'_3, -\psi'_4)^T$$

with energy $-E$.

C.2 Time Reversal Symmetry

The operator defining the time reversal symmetry for nanotubes is given by

$$\mathcal{T}' = (\sigma_0 \otimes \sigma_2)\mathcal{K}. \quad (\text{C.9})$$

Since the Hamiltonian H' commutes with \mathcal{T}' , the spinor

$$\tilde{\psi} = \mathcal{T}'\psi' = (-i\psi'_2, i\psi'_1, -i\psi'_4, i\psi'_3)^T$$

satisfies the eigenvalue equation of H' with energy E too.

C.3 Charge Conjugation

The operator defining charge conjugation for nanotubes is given by

$$\mathcal{C}' = -i(\sigma_2 \otimes \sigma_2)\mathcal{K} \quad (\text{C.10})$$

Since the Hamiltonian H' anticommutes with \mathcal{C}' , the spinor

$$\tilde{\psi} = \mathcal{C}'\psi' = (-i\psi_4'^*, i\psi_3'^*, i\psi_2'^*, -i\psi_1'^*)^T$$

satisfies the eigenvalue equation of H' with energy $-E$.

C.4 Parity

The operator defining parity for nanotubes is given by

$$\mathcal{P}' = \sigma_1 \otimes \sigma_0 \quad (\text{C.11})$$

Since the Hamiltonian H' anticommutes with \mathcal{P}' , the spinor

$$\tilde{\psi} = \mathcal{P}'\psi' = (\psi_3', \psi_4', \psi_1', \psi_2')^T$$

satisfies the eigenvalue equation of H' with energy $-E$.

C.5 Pseudo-Spin-Flip Symmetry

Due to the cylindrical geometry of carbon nanotubes, there exists another kind symmetry; the so-called pseudo-spin-flip symmetry. We refer to pseudo-spin as the intrinsic label defining each sublattice. A flip in this variable implies an interchange of the sites between both sublattices. For CNTs, the axis coincides with the z -axis, thus the symmetry corresponds to make a 180° degree turn around that axis (or a reflection over the x - y plane): $z \rightarrow -z$. The operator defining this symmetry is given by

$$\rho_z = i\sigma_1 \otimes \sigma_3 \quad (\text{C.12})$$

Since the Hamiltonian H' commutes with ρ_z , the spinor

$$\tilde{\psi} = \rho_z \psi' = (i\psi_3'^*, -i\psi_4'^*, i\psi_1'^*, -i\psi_2'^*)^T$$

satisfies the eigenvalue equation of H' with energy E too.

Appendix D

Technical Lemmas

In this appendix, we include the technical lemmas necessary to show the self-adjointness of two-valley four-component Dirac operators on two-dimensional domains. The heuristic approach consists in to reproduce the structure of reference [13] for four-spinors. For simplicity, we only include Dirac operators with boundary conditions conserving (breaking) the electron-hole symmetry. The proof for general boundary conditions, described by the four-parameter family M in (2.8) is straightforward.

Henceforth, we will change the notation of the Dirac operators because of the number of parameters. We (re)define $H(M)$ as the operator acting as H in the domain

$$\mathcal{D}(H(M)) = \{u \in H^1(\Omega, \mathbb{C}^4) \mid P_-(M)\gamma u = 0\},$$

where $P_{\pm}(M) \equiv (1 \pm M)/2$, and M is defined as (2.8) or a particular case of it.

We start with general considerations to introduce the technical lemmas. Next, we proof the self-adjointness in the unit circle. After, we extend the result using Riemann mapping to general planar domains. We finish with the extension of [14], determining the lower bound for the lowest eigenvalue, in absolute value.

D.1 General Considerations

We define

$$\tilde{\mathcal{K}} = \{u \in L^2(\Omega, \mathbb{C}^4) \mid Hu \in L^2(\Omega, \mathbb{C}^4)\}, \quad (\text{D.1})$$

equipped with the graph-norm $\|u\|_{\tilde{\mathcal{K}}} = \|u\|^2 + \|Hu\|^2$. By [13, Lemma 2.1], $\tilde{\mathcal{K}}$ is a Hilbert space and $C^\infty(\bar{\Omega}, \mathbb{C}^4)$ is dense in $\tilde{\mathcal{K}}$. Moreover, by [13, Lemma 2.2], we have that $\mathcal{D}(H^*(M)) \subset \tilde{\mathcal{K}}$ and $\tilde{\mathcal{K}} \subset H_{\text{loc}}^1(\Omega, \mathbb{C}^4)$.

In the following lemma, we show that if a spinor v is in the domain of the adjoint operator of $H(M)$, then it satisfies the condition $P_-(M)\gamma v = 0$. This is an extension of [13, Lemma 2.3].

Lemma D.1. *The trace operator γ extends to a continuous map*

$$\gamma : \tilde{\mathcal{K}} \rightarrow H^{-1/2}(\partial\Omega, \mathbb{C}^4).$$

Moreover,

1. If $v \in \mathcal{D}(H^*(M'_\Lambda))$, then $P_-(M'_\Lambda)\gamma v = 0$. An equivalent formulation is $\gamma v_4 = \left(\frac{1-\sin\Lambda}{\cos\Lambda}\right)\nu t\gamma v_1$ and $\gamma v_3 = \left(\frac{1+\sin\Lambda}{\cos\Lambda}\right)\nu t^*\gamma v_2$.
2. If $v \in \mathcal{D}(H^*(M''_\Lambda))$, then $P_-(M''_\Lambda)\gamma v = 0$. An equivalent formulation is $\gamma v_2 = t \sec \Lambda' \gamma v_1 - t\nu^* \tan \Lambda' \gamma v_3$ and $\gamma v_4 = -t\nu \tan \Lambda' \gamma v_1 + t \sec \Lambda' \gamma v_3$.
3. If $v \in \mathcal{D}(H^*(M_\infty))$, then $P_-(M_\infty)\gamma v = 0$. An equivalent formulation is $\gamma v_1 = t^*\gamma v_2$ and $\gamma v_3 = -t^*\gamma v_4$.

Remark 1. *In the third case, we took the positive version of M_∞ . In the negative version, we have the conditions $\gamma v_1 = -t^*\gamma v_2$ and $\gamma v_3 = t^*\gamma v_4$.*

Remark 2. *For zigzag boundary conditions, the condition $P_-(M_{zz})\gamma v = 0$ implies that two components of the spinor cancel at the boundary, depending on the case.*

Proof Lemma D.1.

The fact that γ extends to a continuous map from $\tilde{\mathcal{K}}$ to $H^{-1/2}(\partial\Omega, \mathbb{C}^4)$ follows straightforwardly from [13, Lemma 2.3].

Let $v \in \mathcal{D}(H^*(M))$ and $u \in \mathcal{D}(H(M))$, then using (2.5) we have that

$$i \int_{\partial\Omega} (\gamma v, \sigma_0 \otimes (\mathbf{n} \cdot \boldsymbol{\sigma}) \gamma u)_{\mathbb{C}^4} = \int_{\Omega} (Hv, u)_{\mathbb{C}^4} - (v, Hu)_{\mathbb{C}^4} = \langle H^*(M)v, u \rangle - \langle v, H(M)u \rangle = 0.$$

Choosing $f = \gamma u = P_+(M)f$ and since by (2.7), it satisfies that $P_+(M)(\sigma_0 \otimes (\boldsymbol{\sigma} \cdot \mathbf{n})) = (\sigma_0 \otimes (\boldsymbol{\sigma} \cdot \mathbf{n}))P_-(M)$. Then,

$$\begin{aligned} (\gamma v, (\sigma_0 \otimes (\boldsymbol{\sigma} \cdot \mathbf{n}))f)_{\mathbb{C}^4} &= (\gamma v, (\sigma_0 \otimes (\boldsymbol{\sigma} \cdot \mathbf{n}))P_+(M)f)_{\mathbb{C}^4}, \\ &= (\gamma v, P_-(M)(\sigma_0 \otimes (\boldsymbol{\sigma} \cdot \mathbf{n}))f)_{\mathbb{C}^4}, \\ &= (P_-(M)\gamma v, (\sigma_0 \otimes (\boldsymbol{\sigma} \cdot \mathbf{n}))f)_{\mathbb{C}^4}. \end{aligned}$$

In the last step, we used that $P_-(M)$ is self-adjoint. Thus, it holds that $P_-(M)\gamma v = 0$. After that, we can write explicitly the matrix M to find the relation between the components of γv in each case.

Case 1.

We compute γv for the case M'_Λ ,

$$\begin{aligned} M'_\Lambda &= ((\boldsymbol{\sigma} \cdot \boldsymbol{\nu}) \otimes (\boldsymbol{\sigma} \cdot \mathbf{t})) \cos \Lambda + (\sigma_0 \otimes \sigma_3) \sin \Lambda, \\ M'_\Lambda &= \begin{pmatrix} 0 & \nu^* \\ \nu & 0 \end{pmatrix} \cos \Lambda \otimes \begin{pmatrix} 0 & t^* \\ t & 0 \end{pmatrix} + \begin{pmatrix} \sigma_3 & 0 \\ 0 & \sigma_3 \end{pmatrix} \sin \Lambda, \\ M'_\Lambda &= \begin{pmatrix} 0 & 0 & 0 & \nu^* t^* \\ 0 & 0 & \nu^* t & 0 \\ 0 & \nu t^* & 0 & 0 \\ \nu t & 0 & 0 & 0 \end{pmatrix} \cos \Lambda + \begin{pmatrix} 1 & 0 & 0 & 0 \\ 0 & -1 & 0 & 0 \\ 0 & 0 & 1 & 0 \\ 0 & 0 & 0 & -1 \end{pmatrix} \sin \Lambda. \end{aligned}$$

Then, for $v = (v_1, v_2, v_3, v_4)^T$, the condition $P_-(M'_\Lambda)\gamma v = 0$ is equivalent to the following system of equations,

$$\begin{aligned} (1 - \sin \Lambda)\gamma v_1 - \cos \Lambda \nu^* t^* \gamma v_4 &= 0, \\ (1 + \sin \Lambda)\gamma v_2 - \cos \Lambda \nu^* t \gamma v_3 &= 0, \\ (1 - \sin \Lambda)\gamma v_3 - \cos \Lambda \nu t^* \gamma v_2 &= 0, \\ (1 + \sin \Lambda)\gamma v_4 - \cos \Lambda \nu t \gamma v_1 &= 0. \end{aligned}$$

These can be rewritten as

$$\gamma v_4 = \left(\frac{1 - \sin \Lambda}{\cos \Lambda} \right) \nu t \gamma v_1 \quad ; \quad \gamma v_3 = \left(\frac{1 + \sin \Lambda}{\cos \Lambda} \right) \nu t^* \gamma v_2 ,$$

or as

$$\gamma v_1 = \left(\frac{1 + \sin \Lambda}{\cos \Lambda} \right) \nu^* t^* \gamma v_4 \quad ; \quad \gamma v_2 = \left(\frac{1 - \sin \Lambda}{\cos \Lambda} \right) \nu^* t \gamma v_3 .$$

We recall that, in the usual convention, the first and fourth components correspond to the spin components of the spinor associated with the sublattice A and the second and third components correspond to the sublattice B . Thus, these boundary conditions only mix the spinor components related to the same sublattice.

Case 2.

We compute γv for the case $M_{\Lambda'}^{\nu}$.

$$M_{\Lambda'}^{\nu} = \begin{pmatrix} 0 & t^* & 0 & 0 \\ t & 0 & 0 & 0 \\ 0 & 0 & 0 & t^* \\ 0 & 0 & t & 0 \end{pmatrix} \cos \Lambda' + \begin{pmatrix} 0 & 0 & \nu^* & 0 \\ 0 & 0 & 0 & -\nu^* \\ \nu & 0 & 0 & 0 \\ 0 & -\nu & 0 & 0 \end{pmatrix} \sin \Lambda' .$$

Then, the condition $P_-(M_{\Lambda'}^{\nu})\gamma v = 0$ is equivalent to the following system of equations,

$$\begin{aligned} \gamma v_1 &= t^* \cos \Lambda' \gamma v_2 + \nu^* \sin \Lambda' \gamma v_3 , \\ \gamma v_2 &= t \cos \Lambda' \gamma v_1 - \nu^* \sin \Lambda' \gamma v_4 , \\ \gamma v_3 &= t^* \cos \Lambda' \gamma v_4 + \nu \sin \Lambda' \gamma v_1 , \\ \gamma v_4 &= t \cos \Lambda' \gamma v_3 - \nu \sin \Lambda' \gamma v_2 . \end{aligned}$$

These can be rewritten as

$$\begin{aligned} \gamma v_2 &= t \sec \Lambda' \gamma v_1 - t \nu^* \tan \Lambda' \gamma v_3 , \\ \gamma v_4 &= -t \nu \tan \Lambda' \gamma v_1 + t \sec \Lambda' \gamma v_3 . \end{aligned}$$

In this case, the boundary conditions mix spinor components of both sublattices.

Case 3.

We compute γv for the case M_∞ .

$$M_\infty = \begin{pmatrix} 0 & t^* & 0 & 0 \\ t & 0 & 0 & 0 \\ 0 & 0 & 0 & -t^* \\ 0 & 0 & -t & 0 \end{pmatrix}.$$

Then, the condition $P_-(M_\infty)\gamma v = 0$ is equivalent to

$$\begin{aligned} \gamma v_1 &= t^* \gamma v_2, \\ \gamma v_3 &= -t^* \gamma v_4. \end{aligned}$$

Again, we notice that the components of the spinor related to different sublattices are mixed, but there is not valley mix. In this case, the mixing is through a rotation around the z -axis due to the phase of the tangent unit vector. \square

D.2 The Unit Circle

Note that Dirac Hamiltonian (1.1) acts as

$$Hu(z) = -2i \begin{pmatrix} 0 & \partial_z & 0 & 0 \\ \partial_{z^*} & 0 & 0 & 0 \\ 0 & 0 & 0 & \partial_z \\ 0 & 0 & \partial_{z^*} & 0 \end{pmatrix} u(z) = -2i \begin{pmatrix} \partial_z u_2(z) \\ \partial_{z^*} u_1(z) \\ \partial_z u_4(z) \\ \partial_{z^*} u_3(z) \end{pmatrix}.$$

Here, we introduced the Cauchy–Riemann derivatives $\partial_z = \frac{1}{2}(\partial_1 - i\partial_2)$ and $\partial_{z^*} = \frac{1}{2}(\partial_1 + i\partial_2)$.

Furthermore, we introduce the Cauchy kernel and its conjugate,

$$\begin{aligned} (Kf)(\zeta) &= \frac{1}{2\pi i} \int_{\partial\Omega} \frac{f(z)}{z - \zeta} d\zeta, \\ (\bar{K}f)(\zeta) &= -\frac{1}{2\pi i} \int_{\partial\Omega} \frac{f(z)}{z^* - \zeta^*} d\zeta^*. \end{aligned}$$

These operators are defined from $C^\infty(\partial\Omega, \mathbb{C})$ to $C^\infty(\partial\Omega, \mathbb{C})$. We construct an operator in $C^\infty(\partial\Omega, \mathbb{C}^4)$ given by

$$\tilde{S} = \sigma_0 \otimes \begin{pmatrix} K & 0 \\ 0 & \bar{K} \end{pmatrix} = \begin{pmatrix} K & 0 & 0 & 0 \\ 0 & \bar{K} & 0 & 0 \\ 0 & 0 & K & 0 \\ 0 & 0 & 0 & \bar{K} \end{pmatrix}. \quad (\text{D.2})$$

On the unit circle \mathbb{S} , the operators K and \bar{K} are explicit when they act on the standard orthonormal basis

$$e_n(\theta) = (2\pi)^{-1/2} e^{in\theta} \in L^2(\mathbb{S}, \mathbb{C}),$$

in the standard parametrization of \mathbb{S} . To prove our next two lemmas, we need the technical result [13, Proposition 2.5], which we reproduce here for completeness. After that, we continue the proof of Theorem 1.1 establishing properties on the unitary disc, $\Omega = \mathbb{D}$ and then finish it for general domains by using the Riemann mapping theorem.

Proposition D.2 (Proposition 2.5, [13]). *If $\Omega = \mathbb{D}$ and K, \bar{K} are defined as above, then for all $s \in [-1/2, 1/2]$*

1. K and \bar{K} extend to bounded operators from $H^{-1/2}(\mathbb{S}, \mathbb{C})$ to $L^2(\mathbb{D}, \mathbb{C})$.
2. For all $f \in H^s(\mathbb{S}, \mathbb{C})$, we have $\partial_z^* K f = 0$ and $\partial_z \bar{K} f = 0$ with derivatives taken in the sense of distributions.
3. γK and $\gamma \bar{K}$ extend to bounded operators on $H^s(\mathbb{S}, \mathbb{C})$, and they are self-adjoint projections onto $\text{span}\{e_n | n \geq 0\}$ and $\text{span}\{e_n | n \leq 0\}$, respectively.
4. $\gamma K + \gamma \bar{K} = 1 + \langle e_0, \cdot \rangle e_0$ when acting on $H^s(\mathbb{S}, \mathbb{C})$.
5. For $\beta \in C^1(\mathbb{S}, \mathbb{C})$ and $s = -1/2$ or $s = 1/2$ the commutators $[\beta, \gamma K]$ and $[\beta, \gamma \bar{K}]$ are bounded from $H^s(\mathbb{S}, \mathbb{C})$ to $H^{s+1/2}(\mathbb{S}, \mathbb{C})$.

Now, using this proposition, we can extend [13, Lemma 2.6] to four-spinors.

Lemma D.3. *Let $\Omega = \mathbb{D}$ and assume $v \in \tilde{\mathcal{K}}$. Then, $\gamma\tilde{\mathcal{S}}((\sigma_0 \otimes \boldsymbol{\sigma} \cdot \mathbf{n})\gamma v) \in H^{1/2}(\mathbb{S}, \mathbb{C}^4)$.*

Proof Lemma D.3.

Let $f \in C^\infty(\mathbb{S}, \mathbb{C}^4)$ and the sequence $(v_n) \in C^1(\bar{\mathbb{D}}, \mathbb{C}^4)$, with $(v_n) \rightarrow v \in \tilde{\mathcal{K}}$. By Proposition D.2 (iii), $\gamma\tilde{\mathcal{S}}$ is self-adjoint. Then,

$$\begin{aligned} -i \int_{\mathbb{S}} \left(\gamma\tilde{\mathcal{S}}((\sigma_0 \otimes \boldsymbol{\sigma} \cdot \mathbf{n})\gamma v_n), f \right)_{\mathbb{C}^4} &= -i \int_{\mathbb{S}} ((\sigma_0 \otimes \boldsymbol{\sigma} \cdot \mathbf{n})\gamma v_n, \gamma\tilde{\mathcal{S}}f)_{\mathbb{C}^4} \\ &= \left\langle v_n, H\tilde{\mathcal{S}}f \right\rangle - \left\langle H\tilde{\mathcal{S}}v_n, f \right\rangle, \end{aligned}$$

where the last term above cancels since, by Proposition D.2 (ii), $H\tilde{\mathcal{S}}f = 0$. Hence, by Cauchy-Schwarz

$$\begin{aligned} \left| \int_{\mathbb{S}} \left(\gamma\tilde{\mathcal{S}}((\sigma_0 \otimes \boldsymbol{\sigma} \cdot \mathbf{n})\gamma v_n), f \right)_{\mathbb{C}^4} \right| &\leq \|Hv_n\|_{L^2(\mathbb{D}, \mathbb{C}^4)} \|\tilde{\mathcal{S}}f\|_{L^2(\mathbb{D}, \mathbb{C}^4)} \\ &\leq C_K \|Hv_n\|_{L^2(\mathbb{S}, \mathbb{C}^4)} \|f\|_{H^{-1/2}(\mathbb{D}, \mathbb{C}^4)}. \end{aligned}$$

In the last step we used Proposition D.2 (i). Taking the limit $n \rightarrow \infty$, we obtain that $\gamma\tilde{\mathcal{S}}((\sigma_0 \otimes \boldsymbol{\sigma} \cdot \mathbf{n})\gamma v)$ extends to a continuous functional on $H^{-1/2}(\mathbb{S}, \mathbb{C}^4)$ and thus, it can be identified with a function in $H^{1/2}(\mathbb{S}, \mathbb{C}^4)$. \square

On the unit circle, the following lemma states that for $v \in \tilde{\mathcal{K}}$ then $\gamma v \in H^{1/2}(\mathbb{S}, \mathbb{C}^4)$.

Lemma D.4. *Let $\Omega = \mathbb{D}$ and $\alpha, \beta \in C^1(\mathbb{S}, \mathbb{C})$ be nowhere vanishing functions. Assume that $v = (v_1, v_2, v_3, v_4)^T \in \tilde{\mathcal{K}}$, and it satisfies one of the following options:*

1. $\gamma v_1 = \beta\gamma v_4$ and $\gamma v_2 = \alpha\gamma v_3$ as an equality in $H^{-1/2}(\mathbb{S}, \mathbb{C})$.
2. $\gamma v_2 = \alpha\gamma v_1 + \beta\nu^*\gamma v_3$ and $\gamma v_4 = \beta\nu\gamma v_1 + \alpha\gamma v_3$ as an equality in $H^{-1/2}(\mathbb{S}, \mathbb{C})$.
3. $\gamma v_1 = \beta\gamma v_2$ and $\gamma v_3 = \alpha\gamma v_4$ as an equality in $H^{-1/2}(\mathbb{S}, \mathbb{C})$.

Then, $\gamma v \in H^{1/2}(\mathbb{S}, \mathbb{C}^4)$.

Remark 3.

1. *In the second case, we can relax the restriction on β , which can be allowed to vanish on \mathbb{S} ; however, the restriction on α is strict.*
2. *In view of Lemma D.1, $v \in \mathcal{D}(H^*(M))$ satisfies the respective hypotheses of Lemma D.4. This implies that $\mathcal{D}(H^*(M)) \subset \mathcal{D}(H(M))$, respectively in each of the three cases.*

3. For zigzag boundary conditions, two components of the spinor v cancel on the boundary. Consequently, we cannot use the completeness argument of operators $\gamma K, \gamma \bar{K}$ to conclude that $\gamma v \in H^{1/2}(\mathbb{S}, \mathbb{C}^4)$.

Proof Lemma D.4.

We define the spinor $f = (\sigma_0 \otimes \boldsymbol{\sigma} \cdot \mathbf{n})\gamma v$. The components of f satisfy

$$f_1 = n^* \gamma v_2 \quad , \quad f_2 = n \gamma v_1 \quad , \quad f_3 = n^* \gamma v_4 \quad , \quad f_4 = n \gamma v_3 . \quad (\text{D.3})$$

Therefore, Lemma D.3 states that

$$\gamma K f_1, \gamma K f_3 \in H^{1/2}(\mathbb{S}, \mathbb{C}) \quad \text{and} \quad \gamma \bar{K} f_2, \gamma \bar{K} f_4 \in H^{1/2}(\mathbb{S}, \mathbb{C}) . \quad (\text{D.4})$$

Case 1.

We have, by Lemma D.1, for the boundary conditions $P_-(M_\Lambda^\nu)\gamma v = 0$,

$$\begin{aligned} \gamma v_1 &= \left(\frac{1 + \sin \Lambda}{\cos \Lambda} \right) \nu^* t^* \gamma v_4 = \beta \gamma v_4 , \\ \gamma v_2 &= \left(\frac{1 - \sin \Lambda}{\cos \Lambda} \right) \nu^* t \gamma v_3 = \alpha \gamma v_3 , \end{aligned}$$

where α, β do not vanish provided that $\cos \Lambda(s) \neq 0$ for all $s \in \mathbb{S}$. Moreover, we note that $\alpha^{-1} = \beta \nu^2$. Therefore, due to the boundary conditions, the components of f satisfy $f_4 = \tilde{\beta} \nu^2 f_1$ and $f_2 = \tilde{\beta} f_3$, where $\tilde{\beta} = n^2 \beta$ is a C^1 -function as well as $\tilde{\beta} \nu^2$.

Now, for f_2 we use (D.3),

$$\gamma K f_2 = \gamma K(\tilde{\beta} f_3) = \tilde{\beta} \gamma K f_3 - [\tilde{\beta}, \gamma K] f_3 .$$

Clearly, the first term is in $H^{1/2}(\mathbb{S}, \mathbb{C})$. Furthermore, by Proposition D.2 (i) and since $\tilde{\beta}$ does not vanish in \mathbb{S} , the second term $[\tilde{\beta}, \gamma K] f_3 \in H^{1/2}(\mathbb{S}, \mathbb{C})$ and the same holds for f_4 . So we obtain that $f \in L^2(\mathbb{S}, \mathbb{C}^4)$, and using the orthogonal complement of the projections, by Proposition D.2 (iv), we conclude that $f \in H^{1/2}(\mathbb{S}, \mathbb{C}^4)$. Finally, since $(\sigma_0 \otimes \boldsymbol{\sigma} \cdot \mathbf{n})^2 = 1$, the same conclusion holds for γv .

Case 2.

By Lemma D.1, we have for boundary conditions $P_-(M'_{\Lambda'})\gamma v = 0$:

$$\begin{aligned}\gamma v_2 &= t \sec \Lambda' \gamma v_1 - t \nu^* \tan \Lambda' \gamma v_3 = \alpha \gamma v_1 + \beta \nu^* \gamma v_3, \\ \gamma v_4 &= -t \nu \tan \Lambda' \gamma v_1 + t \sec \Lambda' \gamma v_3 = \beta \nu \gamma v_1 + \alpha \gamma v_3,\end{aligned}$$

where α, β are $C^1(\mathbb{S}, \mathbb{C})$ nowhere vanishing functions provided that $\cos \Lambda'(s) \neq 0$ for all $s \in \mathbb{S}$. The components of f satisfy:

$$f_1 = (n^*)^2 \alpha f_2 + \nu^* (n^*)^2 \beta f_4 \quad \text{and} \quad f_3 = (n^*)^2 \beta f_2 + \nu (n^*)^2 \alpha f_4.$$

We note that f_1, f_3 are linear combinations of f_2, f_4 with $C^1(\mathbb{S}, \mathbb{C})$ nowhere vanishing functions. Therefore, we can proceed in the same way as in the previous case to show that $\gamma \bar{K} f_1, \gamma \bar{K} f_3 \in H^{1/2}(\mathbb{S}, \mathbb{C})$, do the same with $\gamma K f_2, \gamma K f_4 \in H^{1/2}(\mathbb{S}, \mathbb{C})$ and conclude that $\gamma v \in H^{1/2}(\mathbb{S}, \mathbb{C}^4)$. If $\sin \Lambda' = 0$, i.e., $\beta = 0$, we conclude that $\gamma v \in H^{1/2}(\mathbb{D}, \mathbb{C}^4)$ through the same procedure given below in the infinity mass case.

Case 3.

By Lemma D.1 we have for M_∞ ,

$$\begin{aligned}\gamma v_1 &= t^* \gamma v_2 = \beta \gamma v_2, \\ \gamma v_3 &= -t^* \gamma v_4 = -\beta \gamma v_4.\end{aligned}$$

We just have $\beta = -\alpha = t^*$ which clearly are $C^1(\mathbb{S}, \mathbb{C})$ nowhere vanishing functions. The components of f satisfy that $f_2 = n^2 t^* f_1 = \tilde{\beta} f_1$ and $f_3 = -n^2 t^* f_4 = -\tilde{\beta} f_4$. Finally, we can follow the same steps given in the case 1 for f_2, f_4 and conclude that $\gamma v \in H^{1/2}(\mathbb{S}, \mathbb{C}^4)$. \square

D.3 Riemann Mapping and the Self-adjointness Proof

Since $\partial\Omega$ is a C^2 -boundary, there exists a C^1 conformal mapping $F : \bar{\Omega} \rightarrow \bar{\mathbb{D}}$ with inverse G [39, Theorem 3.5, p. 48]. Consider the map U defined by $(Uf)(z) = f(G(z))$ mapping functions on $\bar{\Omega}$ to functions on $\bar{\mathbb{D}}$. Furthermore, U also maps functions on $\partial\Omega$ to functions on \mathbb{S} . By [13, Lemma 2.8] $U : L^2(\Omega) \rightarrow L^2(\mathbb{D})$ is bounded with bounded inverse. Moreover, U defines a

bounded bijection from $H^s(\partial\Omega)$ to $H^s(\mathbb{S})$ with bounded inverse, for all $s \in [-1, 1]$.

Lemma D.5. *When Ω is simply connected and has C^2 -boundary, we define U as above, also*

1. *If $v \in \mathcal{D}(H^*(M_\Lambda^\nu))$, then $Uv = (u_1, u_2, u_3, u_4)^T \in \tilde{K}(\mathbb{D})$ and on the boundary $\gamma v_1 = \beta \gamma v_4$ and $\gamma v_2 = \alpha \gamma v_3$ as identities in $H^{-1/2}(\mathbb{S})$, where $\alpha = U\left(\frac{\nu t^* \cos \Lambda}{1 - \sin \Lambda}\right)$ and $\beta = U\left(\frac{\nu t \cos \Lambda}{1 - \sin \Lambda}\right)$ are $C^1(\mathbb{S}, \mathbb{C})$.*
2. *If $v \in \mathcal{D}(H^*(M_{\Lambda'}^\nu))$, then $Uv = (u_1, u_2, u_3, u_4)^T \in \tilde{K}(\mathbb{D})$ and on the boundary $\gamma v_2 = \alpha \gamma v_1 + \beta \nu^* \gamma v_3$ and $\gamma v_4 = \beta \nu \gamma v_1 + \alpha \gamma v_3$ as identities in $H^{-1/2}(\mathbb{S})$, where $\alpha = U(t \sec \Lambda')$ and $\beta = -U(t \tan \Lambda')$ are $C^1(\mathbb{S}, \mathbb{C})$.*
3. *If $v \in \mathcal{D}(H^*(M_\infty))$, then $Uv = (u_1, u_2, u_3, u_4)^T \in \tilde{K}(\mathbb{D})$ and on the boundary $\gamma v_1 = \beta \gamma v_2$ and $\gamma v_3 = \alpha \gamma v_4$ as identities in $H^{-1/2}(\mathbb{S})$, where $\alpha = Ut^*$ and $\beta = -Ut^*$ are $C^1(\mathbb{S}, \mathbb{C})$.*

Proof Lemma D.5.

Assume $v = (v_1, v_2, v_2, v_2)^T$ is in the corresponding $\mathcal{D}(H^*(M))$. Then, since $\partial_{z^*} G = 0$, we have by the chain rule,

$$\begin{aligned} \partial_z u_2 &= G' \partial_z v_2 \in L^2(\mathbb{D}, \mathbb{C}), & \partial_{z^*} u_1 &= (G')^* \partial_{z^*} v_2 \in L^2(\mathbb{D}, \mathbb{C}), \\ \partial_z u_4 &= G' \partial_z v_4 \in L^2(\mathbb{D}, \mathbb{C}), & \partial_{z^*} u_3 &= (G')^* \partial_{z^*} v_3 \in L^2(\mathbb{D}, \mathbb{C}). \end{aligned}$$

Finally, the corresponding boundary conditions for u follow from the boundary conditions satisfied by v given in Lemma D.1. □

Self-Adjointness Proof

We only show the simply connected case because the multiply connected case is straightforward by [13].

Simply connected case. Let $v \in \mathcal{D}(H^*(M))$. By Lemma D.1, we only have to prove that $\gamma v \in H^{1/2}(\partial\Omega, \mathbb{C}^4)$. By Lemma D.5, this is equivalent to show that $\gamma u = \gamma Uv \in H^{1/2}(\mathbb{S}, \mathbb{C}^4)$, where U is the map defined above. Furthermore, $u \in \tilde{K}(\mathbb{D})$ and its components u_1, u_2, u_3, u_4 satisfy the boundary conditions given in Lemma D.5. Since the corresponding functions α and β vanish nowhere by assumption, we can apply Lemma D.4 and conclude the proof.

D.4 Spectral Gaps of Dirac Hamiltonians

We take the boundary conditions associated with the matrix

$$M'_\Lambda = \sin \Lambda (\sigma_0 \otimes \sigma_3) + \cos \Lambda ((\boldsymbol{\sigma} \cdot \boldsymbol{\nu}) \otimes (\boldsymbol{\sigma} \cdot \boldsymbol{t})).$$

Then, we have the following lemma concerning $H(M'_\Lambda)$.

Lemma D.6. *Take $H(M'_\Lambda)$ satisfying the hypotheses of Theorem 3.1. If λ is the eigenvalue of $H(M'_\Lambda)$ of smallest absolute value, then it satisfies*

$$\lambda^2 \geq B_\Lambda^2 \lambda_0^2,$$

with B_Λ defined as (1.9) and λ_0 the first positive eigenvalue of the operator with $\Lambda = 0$.

Proof Lemma D.6.

Assume $\Lambda \in (0, \pi/2)$ such that $B_\Lambda = (1 - \sin \Lambda) / \cos \Lambda \in (0, 1)$. Take an eigenspinor u of $H(M'_\Lambda)$ associated with the eigenvalue λ . Because of the boundary conditions $P_-(M'_\Lambda)\gamma u = 0$, we obtain that $\gamma u_4 = B_\Lambda \nu t \gamma u_1$ and $\gamma u_2 = B_\Lambda \nu^* t \gamma u_3$. Then, we write $u = v + w$, such that

$$v = \sigma_0 \otimes \begin{pmatrix} B_\Lambda & 0 \\ 0 & 1 \end{pmatrix} u \quad \text{and} \quad w = \sigma_0 \otimes \begin{pmatrix} 1 - B_\Lambda & 0 \\ 0 & 0 \end{pmatrix} u.$$

We have that $v \in \mathcal{D}(H(M'_{\Lambda=0}))$ and $w \in \mathcal{D}(H(M'_{\Lambda=\pi/2}))$. Now,

$$\lambda^2 \|u\|^2 = \langle Hu, Hu \rangle = \|Hv\|^2 + \|Hw\|^2 + 2 \operatorname{Re} \langle Hv, Hw \rangle.$$

We compute:

$$\begin{aligned} \|Hw\|^2 &= (1 - B_\Lambda)^2 \left(\|(-i\partial_1 - \partial_2)u_1\|^2 + \|(-i\partial_1 - \partial_2)u_3\|^2 \right), \\ \langle Hv, Hw \rangle &= B_\Lambda(1 - B_\Lambda) \left(\|(-i\partial_1 - \partial_2)u_1\|^2 + \|(-i\partial_1 - \partial_2)u_3\|^2 \right), \\ \|Hv\|^2 &= \|H(M'_{\Lambda=0})v\|^2 \geq \lambda_0^2 \|v\|^2 \geq \lambda_0^2 B_\Lambda^2 \|u\|^2. \end{aligned}$$

The last inequality holds because $|B_\Lambda| \leq 1$. Using this fact and combining the terms which

include w , we obtain

$$\begin{aligned}\lambda^2\|u\|^2 &= \|Hv\|^2 + (1 - B_\Lambda^2)\left(\|(-i\partial_1 - \partial_2)u_1\|^2 + \|(-i\partial_1 - \partial_2)u_3\|^2\right) \\ &\geq \lambda_0^2 B_\Lambda^2 \|u\|^2\end{aligned}$$

which is the desired inequality. The other cases are analogous: it suffices to define $v = \sigma_0 \otimes \begin{pmatrix} -B_\Lambda & 0 \\ 0 & 1 \end{pmatrix} u$ when $\Lambda \in (\pi/2, \pi)$ or $v = \sigma_0 \otimes \begin{pmatrix} 1 & 0 \\ 0 & \pm B_\Lambda \end{pmatrix} u$ for $\Lambda \in (\pi, 3\pi/2)$ and $\Lambda \in (3\pi/2, 2\pi)$, respectively. \square

Proof of Corollary 4.1.

By the previous lemma, our problem is restricted to $\Lambda = 0$, so we focus our attention on finding a lower bound to the eigenvalue of smallest absolute value λ_0 of the operator $H(M'_{\Lambda=0})$. Let $u, v \in \mathcal{D}(H(M'_{\Lambda=0}))$, integrating by parts and using the (anti)commutation relation of the Pauli matrices, we obtain

$$(H(M'_{\Lambda=0})u, H(M'_{\Lambda=0})v) = \int_{\Omega} (\nabla u, \nabla v)_{\mathbb{C}^4} + i \int_{\partial\Omega} (u, (\sigma_0 \otimes \sigma_3) \mathbf{t} \cdot \nabla v)_{\mathbb{C}^4}.$$

We can explicitly write out the spinor components and introduce the boundary conditions $u_4 = \nu t u_1$ and $u_2 = \nu^* t u_3$,

$$\begin{aligned}(u, (\sigma_0 \otimes \sigma_3) \mathbf{t} \cdot \nabla v)_{\mathbb{C}^4} &= u_1^* \mathbf{t} \cdot \nabla v_1 - u_2^* \mathbf{t} \cdot \nabla v_2 + u_3^* \mathbf{t} \cdot \nabla v_3 - u_4^* \mathbf{t} \cdot \nabla v_4, \\ &= -u_1^* v_1 t^* t' - u_3^* v_3 t^* t' \\ &= -i\kappa(s)[u_1^* v_1 + u_3^* v_3] \\ &= -\frac{i}{2}\kappa(s)(u, v)_{\mathbb{C}^4}.\end{aligned}$$

In the second equality, we used $\partial_s \mathbf{t}(s) = -\kappa(s) \mathbf{n}(s)$, with $\kappa(s)$ the curvature. Therefore,

$$(H(M'_{\Lambda=0})u, H(M'_{\Lambda=0})v) = (\nabla u, \nabla v) + \frac{1}{2} \int_{\partial\Omega} (u, v)_{\mathbb{C}^4}(s) \kappa(s) ds.$$

Following the same calculations as in [14, p.6–7] one gets $\lambda_0^2 \geq 2\pi/|\Omega|$. Finally, using Lemma D.6, we conclude that $\lambda^2 \geq B_\Lambda^2(2\pi)/|\Omega|$. \square

Next, we consider the boundary conditions associated with the matrix

$$M_{\Lambda'}^{\nu} = \cos \Lambda' (\sigma_0 \otimes (\boldsymbol{\sigma} \cdot \mathbf{t})) + \sin \Lambda' ((\boldsymbol{\sigma} \cdot \boldsymbol{\nu}) \otimes \sigma_3),$$

where $|\nu| = 1$. Using a unitary transformation, as explained below, one can transform this into a analog case discussed above for M_{Λ}^{ν} .

Lemma D.7. *Take $H(M_{\Lambda'}^{\nu})$ satisfying the hypotheses of Theorem 3.1. If λ is the eigenvalue of $H(M_{\Lambda'}^{\nu})$ of smallest absolute value, then it satisfies*

$$\lambda^2 \geq B_{\Lambda'}^2 \lambda_0^2.$$

with $B_{\Lambda'}$ defined as (1.9), and λ_0 is the he first positive eigenvalue of the operator with $\Lambda' = 0$.

Proof Lemma D.7.

Define the unitary transformation given by the matrix $\tilde{U}_{\nu} = U_{\phi=\pi} U_{\nu}$, where

$$U_{\nu} = \begin{pmatrix} \nu \sigma_0 & 0 \\ 0 & \sigma_0 \end{pmatrix} \quad \text{and} \quad U_{\phi=\pi} = \frac{1}{\sqrt{2}} \begin{pmatrix} 1 & 1 \\ -1 & 1 \end{pmatrix} \otimes \sigma_0.$$

Using the unitary matrix U_{ν} , we can restrict our attention to the case $\nu = 1$. The unitary matrix $U_{\phi=\pi/2}$, defined in (3.4), diagonalizes the second term of $M_{\Lambda'}^{\nu}$, and keeps invariant the first matrix term. This unitary matrix transforms the mixing matrix into

$$\tilde{M}_{\Lambda'} \equiv \tilde{U}_{\nu} M_{\Lambda'}^{\nu} \tilde{U}_{\nu}^* = (\sigma_0 \otimes \boldsymbol{\sigma} \cdot \mathbf{t}) \cos \Lambda' + (\sigma_3 \otimes \sigma_3) \sin \Lambda', \quad (\text{D.5})$$

and the Hamiltonian keeps invariant.

By Theorem 3.1, the corresponding operator $H(\tilde{M}_{\Lambda'})$ is self-adjoint provided that $\cos \Lambda' \neq 0$ at $\partial\Omega$. By definition, for $u \in H(M_{\Lambda'}^{\nu})$, it holds

$$\begin{aligned} \lambda^2 \|u\|^2 &= \langle Hu, Hu \rangle = \langle \tilde{U}_{\nu} H \tilde{U}_{\nu}^* u, \tilde{U}_{\nu} H \tilde{U}_{\nu}^* u \rangle \\ &= \langle H\tilde{u}, H\tilde{u} \rangle = \|H\tilde{u}\|^2, \end{aligned}$$

with $\tilde{u} = \tilde{U}_{\nu} u$ in the domain of $H(\tilde{M}_{\Lambda'})$.

Assuming $\Lambda' \in (0, \pi/2)$, $B_{\Lambda'} = (1 - \sin \Lambda') / \cos \Lambda' \in (0, 1)$. Writing out the boundary conditions explicitly, we obtain $\gamma \tilde{u}_2 = B_{\Lambda'} t \gamma \tilde{u}_1$ and $\gamma \tilde{u}_3 = B_{\Lambda'} t^* \gamma \tilde{u}_4$. Then, we may write

$\tilde{u} = \tilde{v} + \tilde{w}$, where

$$\tilde{v} = \text{diag}\{1, B_{\Lambda'}, B_{\Lambda'}, 1\}\tilde{u} \quad \text{and} \quad \tilde{w} = \text{diag}\{0, 1 - B_{\Lambda'}, 1 - B_{\Lambda'}, 0\}\tilde{u}.$$

This gives $\tilde{v} \in \mathcal{D}(H(\widetilde{M}_{\Lambda'=0}))$ and $\tilde{w} \in \mathcal{D}(H(\widetilde{M}_{\Lambda'=\pi/2}))$. Now, we compute

$$\begin{aligned} \|H\tilde{w}\|^2 &= (1 - B_{\Lambda'})^2 \left(\|(-i\partial_1 - \partial_2)\tilde{u}_2\|^2 + \|(-i\partial_1 + \partial_2)\tilde{u}_3\|^2 \right) \\ \langle H\tilde{v}, H\tilde{w} \rangle &= B_{\Lambda'}(1 - B_{\Lambda'}) \left(\|(-i\partial_1 - \partial_2)\tilde{u}_2\|^2 + \|(-i\partial_1 + \partial_2)\tilde{u}_3\|^2 \right) \\ \|H\tilde{v}\|^2 &= \left\| H(\widetilde{M}_{\Lambda'=0})\tilde{v} \right\|^2 \geq \lambda_0^2 \|\tilde{v}\|^2 \geq \lambda_0^2 B_{\Lambda'}^2 \|u\|^2 \end{aligned}$$

Using this, we analogously obtain that

$$\lambda^2 \geq \lambda_0^2 B_{\Lambda'}^2.$$

Here, λ_0 is the eigenvalue of $H(M_{\Lambda'=0}^\nu)$ of smallest absolute value. The other cases are analogous: it suffices to define $\tilde{v} = \text{diag}\{1, -B_{\Lambda'}, -B_{\Lambda'}, 1\}\tilde{u}$ when $\Lambda' \in (\pi/2, \pi)$ or $\tilde{v} = \text{diag}\{\pm B_{\Lambda'}, 1, 1, \pm B_{\Lambda'}\}\tilde{u}$ for $\Lambda' \in (\pi, 3\pi/2)$ and $\Lambda' \in (3\pi/2, 2\pi)$, respectively. \square

Proof of Corollary 4.2.

By the previous lemma, our problem is restricted to $\Lambda' = 0$, so we focus our attention on finding a lower bound to the eigenvalue of smallest absolute value λ_0 of the operator $H(M_{\Lambda'=0}^\nu)$. Let $u, v \in \mathcal{D}(H(M_{\Lambda'=0}^\nu))$, integrating by parts and using the (anti)commutation relation of the Pauli matrices, we obtain

$$(H(M_{\Lambda'=0}^\nu)u, H(M_{\Lambda'=0}^\nu)v) = \int_{\Omega} (\nabla u, \nabla v)_{\mathbb{C}^4} + i \int_{\partial\Omega} (u, (\sigma_0 \otimes \sigma_3) \mathbf{t} \cdot \nabla v)_{\mathbb{C}^4}.$$

We can explicitly write out the spinor components and introduce the boundary conditions $u_4 = tu_3$ and $u_2 = tu_1$,

$$(u, (\sigma_0 \otimes \sigma_3) \mathbf{t} \cdot \nabla v)_{\mathbb{C}^4} = -i\kappa(s)[u_1^* v_1 + u_3^* v_3].$$

Therefore,

$$(H(M_{\Lambda'=0}^\nu)u, H(M_{\Lambda'=0}^\nu)v) = (\nabla u, \nabla v) + \frac{1}{2} \int_{\partial\Omega} (u, v)_{\mathbb{C}^4}(s)\kappa(s) ds.$$

Again, following the same calculations as in [14, p.6–7] one gets $\lambda_0^2 \geq 2\pi/|\Omega|$. Finally, using Lemma D.7, we conclude that $\lambda^2 \geq B_\Lambda^2(2\pi)/|\Omega|$. \square

Bibliography

- [1] Abanin, D., Lee, P., Levitov, L.: Spin Filtered Edge States and Quantum Hall Effect in Graphene. *Phy. Rev. Lett.* **96**, 176803 (2006).
- [2] Abanin, D., Lee, P., Levitov, L.: Charge and Spin Transport at the Quantum Hall Edge of Graphene. *Solid State Commun.* **143**, 77–85 (2007).
- [3] Akhmerov, A. R., Beenakker, C. W. J.: Detection of Valley Polarization in Graphene by a Superconducting Contact. *Phys. Rev. Lett.* **98**, 157003 (2007).
- [4] Akhmerov, A. R., Beenakker, C. W. J.: Boundary conditions for Dirac fermions on a terminated honeycomb lattice. *Phys. Rev. B* **77**, 085423 (2008).
- [5] Ando, T.: Theory of electronic states and transport in carbon nanotube. *J. Phys. Soc. Jpn.* **74**, 777–817 (2005).
- [6] Arrizabalaga, N., Le Treust, L., Raymond, N.: On the MIT bag model in the non-relativistic limit. *Commun. Math. Phys.* **354**, 641–669 (2017).
- [7] Arrizabalaga, N., Le Treust, L., Mas, A., Raymond, N.: The MIT bag model as an infinite mass limit. *Journal de l’Ecole Polytechnique – Mathématiques*, Tome **6**, 329–365 (2019).
- [8] Barbaroux, JM., Cornean, H., Le Treust, L., Stockmeyer, E.: Resolvent Convergence to Dirac Operators on Planar Domains. *Ann. Henri Poincaré* **20**, 1877–1891 (2019).
- [9] Bär, C.: Lower eigenvalue estimates for Dirac operators. *Math. Ann.* **293**, 1, 39–46 (1992).
- [10] Behrndt, J., Exner, P., Holzmann, M., Lotoreichik, V.: On the spectral properties of Dirac operators with electrostatic δ -shell interactions. *J. Math. Pures Appl.* (9) **111**: 47–78 (2018).

- [11] Behrndt, J., Exner, P., Holzmann, M., Lotoreichik, V.: On Dirac operators in \mathbb{R}^3 with electrostatic and Lorentz scalar δ -shell interactions. *Quantum Stud. Math. Found.* **6**, 295–314 (2019).
- [12] Behrndt, J., Holzmann, M., Mas, A.: Self-Adjoint Dirac Operators on Domains in \mathbb{R}^3 . *Annales Henri Poincaré*, **21**(8), 2681–2735 (2020).
- [13] Benguria, R. D., Fournais, S., Stockmeyer, E., Van Den Bosch, H.: Self-Adjointness of Two-Dimensional Dirac Operators on Domains. *Ann. Henri Poincaré* **18**, 1371–1383 (2017).
- [14] Benguria, R. D., Fournais, S., Stockmeyer, E., Van Den Bosch, H.: Spectral Gaps of Dirac Operators Describing Graphene Quantum Dots. *Math. Phys. Anal. Geom.* **20**, 11 (2017).
- [15] Benhellal, B.: Spectral Asymptotic for the Infinite Mass Dirac Operator in bounded domain (2019). Preprint: [arXiv:1909.03769](https://arxiv.org/abs/1909.03769)
- [16] Berry, M. V., Mondragon, R. J.: Neutrino billiards: time-reversal symmetry-breaking without magnetic fields. *Proc. R. Soc. London A* **412**, 53–74 (1987).
- [17] Borrelli, W.: Multiple solutions for a self-consistent Dirac equation in two dimensions. *Journal of Mathematical Physics*, **59**(4), 041503 (2018).
- [18] Brey, L., Fertig, H. A.: Electronic states of graphene nanoribbons studied with the Dirac equation, *Phys. Rev. B* **73**, 235411 (2006).
- [19] Cassano, B., Lotoreichik, V.: Self-adjoint extensions of the two-valley Dirac operator with discontinuous infinite mass boundary conditions. To appear in *Oper. Matrices* (2020).
- [20] Castro Neto, A. H., Guinea, F., Peres, N. M. R., Novoselov, K. S., Geim, A. K.: The electronic properties of graphene, *Rev. Mod. Phys.* **81**, 109–162 (2009).
- [21] DiVincenzo, D. P., Mele, E. J.: Self-consistent effective-mass theory for intralayer screening in graphite intercalation compounds. *Phys. Rev. B*, **29**(4), 1685–1694 (1984).
- [22] Dresselhaus, S., Dresselhaus, G., Avouris, P.: *Carbon Nanotube Synthesis, Structure, Properties and Applications*. Springer (2001).
- [23] Fathi, D.: A review of electronic band structure of graphene and carbon nanotubes using tight binding. *Journal of Nanotechnology*, **2011**, 1–6 (2011).

-
- [24] Fefferman, C. L., Weinstein, M.: Honeycomb lattice potentials and Dirac points. *J. Amer. Math. Soc.* **25**, 1169–1220 (2012).
- [25] Freitas, P., Siegl, P.: Spectra of graphene nanoribbons with armchair and zigzag boundary conditions. *Rev. Math. Phys.* **26**(10), 1450018 (2014).
- [26] Geim, A.K., Novoselov, K.S.: The rise of graphene. *Nat. Matter*, **6**, 183–191 (2007).
- [27] Holtzmann, M.: A note on the three dimensional Dirac operator with zigzag type boundary conditions (2020). Preprint: <https://arxiv.org/abs/2006.16739>
- [28] Imani Yengejeh, S., Kazemi, S.A., Öchsner, A.: *Geometric Definitions: A Primer on the Geometry of Carbon Nanotubes and Their Modifications*. SpringerBriefs in Applied Sciences and Technology. Springer (2015).
- [29] Javey, A., Kong J.: *Carbon Nanotube Electronics*. Springer, New York, NY, USA (2009).
- [30] Le Treust, L., Ourmières-Bonafos, T.: Self-adjointness of Dirac operators with infinite mass boundary conditions in sectors. *Annales Henri Poincaré*, **19**(5): 1465–1487 (2018).
- [31] Lotoreichik, V., Ourmières-Bonafos, T.: A sharp upper bound on the spectral gap for graphene quantum dots. *Math. Phys. Anal. Geom.* **22**, 13 (2019).
- [32] McCann, E., Fal’ko, V. I.: Symmetry of boundary conditions of the Dirac equation for electrons in carbon nanotubes. *J. Phys. Condens. Matter* **16**(13), 2371–2379 (2004).
- [33] Mina, A., Awadallah, A., Phillips, A.: Simulation of the Band Structure of Graphene and Carbon Nanotube. *Journal of Physics: Conference Series* **343**, 012076 (2012).
- [34] Moroianu, A., Ourmières-Bonafos, T., Pankrashkin, K.: Dirac Operators on Hypersurfaces as Large Mass Limits. *Commun. Math. Phys.* **374**, 1963–2013 (2020).
- [35] Moser, B. K.: *Linear Models: A Mean Model Approach (Probability and Mathematical Statistics)*. Springer, New York (1996).
- [36] Novoselov, K., Geim, A., Morozov, S., Jiang, D., Zhang, Y., Dubonos, S., Gigorieva, I., Firsov, A.: Electric field effect in atomically thin carbon films. *Science*, **306**, 666–669 (2004).
- [37] Orlof, A., Ruseckas, J., Zozoulenko, I.V.: Effect of zigzag and armchair edges on the electronic transport in single-layer and bilayer graphene nanoribbons with defects, *Phys. Rev. B* **88**, 125409 (2013).

- [38] Pizzichillo, F., Van Den Bosch, H.: Self-adjointness of two dimensional Dirac operators on corner domains (2019). Preprint: [arXiv:1902.05010](https://arxiv.org/abs/1902.05010).
- [39] Pommerenke, Ch.: Boundary behaviour of conformal maps. In: Grundlehren der mathematischen Wissenschaften [A Series of Comprehensive Studies in Mathematics]. Springer, Berlin (1991).
- [40] Ponomarenko, L. A., Schedin, F., Katsnelson, M. I., Yang, R., Hill, E. W., Novoselov, K. S., Geim, A. K.: Chaotic Dirac billiard in graphene quantum dots. *Science* **320**, 356–358 (2008).
- [41] Poole, C.P., Owens, F.J.: Introduction to Nanotechnology. John Wiley & Sons (2003).
- [42] Porter, C-E.: Statistical theories of spectra: Fluctuations. Academic Press, New York (1965).
- [43] Rafii-Tabar, H.: Computational Physics of Carbon Nanotubes. Cambridge University Press, Cambridge, UK, 1st edition (2008).
- [44] Saito, R., Dresselhaus, M.S., Dresselhaus, G.: Physical Properties of Carbon Nanotubes. Imperial College Press, London, UK (2004).
- [45] Sakurai, J. J.: Modern Quantum Mechanics. USA: Benjamin (1985).
- [46] Schmidt, K. M.: A remark on boundary value problems for the Dirac operator. *Q. J. Math. Oxf. Ser. (2)* **46**, 509–516 (1995).
- [47] Semenoff, G.W.: Condensed-Matter Simulation of a Three-Dimensional Anomaly. *Phys. Rev. Lett.* **53**, 2449–2452 (1984).
- [48] Stockmeyer, E., Vugalter, S.: Infinite mass boundary conditions for Dirac operators. *Journal of Spectral Theory* **9**(2), 569–600 (2019).
- [49] Wallace, P. R.: The band theory of graphite. *Phys. Rev.* **71** (9), 622–634 (1947).
- [50] Zheng, H., Wang, Z.F., Luo, T., Shi, Q. W., Chen, J.: Analytical study of electronic structure in armchair graphene nanoribbons. *Phys. Rev. B* **75**, 165414 (2007).